Event-Triggered Quantized Control for Input-to-State Stabilization of Linear Systems With Distributed Output Sensors

Mahmoud Abdelrahim, *Member, IEEE*, Victor Sebastiaan Dolk, *Student Member, IEEE*, and W. P. M. H. Heemels, *Fellow, IEEE*

***Abstract*—We study output-based stabilization of linear time-invariant systems affected by unknown external disturbances. The plant outputs are measured by a collection of distributed sensors, which transmit their feedback information to the controller in an asynchronous fashion over different digital communication channels. Before transmission of measurements is possible quantization is needed, which is carried out by means of dynamic quantizers. To save valuable communication resources, the transmission instants of each sensor are determined by event-triggering mechanisms that only depend on locally available information. We propose a systematic methodology for the joint design of the (distributed) dynamic quantizers and the event-triggering mechanisms ensuring an input-to-state stability property of a size-adjustable set around the origin. Moreover, the proposed approach prevents the occurrence of Zeno behavior on the transmission instants and on the updates of the quantizer variable thereby guaranteeing that a finite number of data is transmitted within each finite time window. The tradeoff between transmissions and quantization is characterized in terms of the design parameters. The method is feasible for any stabilizable and detectable linear plant. The systematic design procedure and the effectiveness of the approach are illustrated on a numerical example.**

***Index Terms*—Event-triggered control (ETC), linear time-invariant (LTI), networked control systems (NCS), zeno behavior.**

Manuscript received November 1, 2018; revised November 5, 2018; accepted February 10, 2019. Date of publication February 19, 2019; date of current version December 3, 2019. This work was supported in part by the Innovational Research Incentives Scheme through "Wireless control systems: A new frontier in automation" under the VICI Grant 11382 and in part by the Netherlands Organisation for Scientific Research (NWO) through the Research Programme "Integrated design approach for safety-critical real-time automotive systems" under Grant 12698. Recommended by Associate Editor S. Tarbouriech. *(Corresponding author: Mahmoud Abdelrahim.)*

M. Abdelrahim is with the Control Systems Technology Group, Department of Mechanical Engineering, Eindhoven University of Technology, The Netherlands, and also with the Department of Mechanical Engineering, Assiut University, Assiut 71515, Egypt (e-mail: m.abdelrahim@aun.edu.eg).

V. S. Dolk and W. P. M. H. Heemels are with the Control Systems Technology Group, Department of Mechanical Engineering, Eindhoven University of Technology, 5612 AZ Eindhoven, The Netherlands (e-mail: v.s.dolk@tue.nl; m.heemels@tue.nl).

Color versions of one or more of the figures in this paper are available online at http://ieeexplore.ieee.org.

Digital Object Identifier 10.1109/TAC.2019.2900338

I. Introduction

THE increasing popularity of networked control systems (NCS) has motivated an extensive research effort in the last two decades. In NCS, the sensors, the controllers, and the actuators interact with each other over shared communication channels. This configuration offers several advantages compared to dedicated point-to-point connections in terms of increased flexibility, lower cost, and ease of maintenance. However, the communication resources of the network are often limited, which induces new challenges on the design of control systems [1]–[3]. In this context, event-triggered control (ETC) schemes have been proposed in the literature as an alternative to traditional time-triggered platforms. The idea of ETC is to generate transmission events based on locally available output measurements of the system instead of purely on time as in most traditional digital control setups. In this way, unnecessary access to the network can be prevented, leading to more efficient usage of the communication resources, see, e.g., [4]–[6] and the references therein. One of the main difficulties in the synthesis of event-triggering conditions is to guarantee appropriate stability/performance properties while preventing the occurrence of Zeno (an infinite number of transmissions in finite time); certainly when only the plant output is available for feedback instead of the full state [7] and/or when the control system is subject to exogenous inputs [8].

Besides reducing the amount of transmissions over the network, quantization is another important and challenging aspect in NCS [9]–[12]. The use of quantization is unavoidable due to the digital nature of the communication channel and the fact that only a finite amount of data can be transmitted over the network. Quantization requires a careful handling as well since the closed-loop stability may no longer be guaranteed when state or output measurements are quantized with insufficient number of quantization regions, see, e.g., [13] and the references therein. Most existing techniques reported in the literature are developed for static quantizers in which the quantizer range and the quantizer error bound are fixed. Therefore, to guarantee that the feedback information remains within range of the static quantizer, i.e., to make sure that the quantizer does not saturate, it is often assumed in the analysis of static quantizers that the quantizer range is infinite [12], [14]. This requirement is impractical due to the finite size of the transmitted data packages. To overcome

this requirement, Brockett *et al.* [15] have proposed to dynamically adjust the quantizer range and the quantizer error bound according to the available feedback information, which leads to so-called dynamic quantizers. To that end, a zoom variable is used to either increase the quantizer range to avoid saturation (referred to as the zoom-out stage) or decrease the quantizer range to extract more precise information (referred to as the zoom-in stage). As such, with dynamic quantizers, quantizer saturation can be avoided while using only a small number of quantization regions (and thus less number of bits need to be communicated), which show their advantages over static quantizers. However, the use of dynamic quantizers also introduce various design challenges. For instance, since the zoom actions are state dependent, the accumulation of zoom instants need to be avoided. Moreover, chattering between the zoom-in and the zoom-out stages should be prevented, and the zoom variable should remain bounded, see also, e.g., [16].

In this paper, we consider the joint design of event-triggering conditions and dynamic quantizers for the purpose of the robust stabilization of linear time-invariant (LTI) systems. The plant may be affected by external disturbances and, as in many applications, only the output of the plant can be measured and not the full state. These output measurements are assumed to be distributed, i.e., they are collected by multiple network nodes and are asynchronously transmitted over different channels. Each of these network nodes employs an event-triggering condition, which only depends on locally available information, to decide when to transmit measurement data. It is important to emphasize that when event triggering and dynamic quantization for encoding the measured values are considered in NCS, the combined analysis becomes more complicated since the design of the event-triggering mechanism and the quantizer are directly coupled. For instance, the sampling-induced error of the feedback information is in general not reset to zero at each transmission instant, as is common in event-triggering results, e.g., [5], [17], due to the effect of quantization [9]–[11]. This issue will have negative impact on the closed-loop stability if not handled properly in the joint design. The handling of this behavior is far from trivial. Moreover, it is desirable in practice that the combined event-triggering mechanism and the dynamic quantizer for each node are designed such that, at each transmission instant, the transmitted information is more accurate with respect to the current output measurement than the information already available at the receiving node. Obviously, the latter is important to avoid redundant usage of the network. Finally, we deal with this delicate co-design problem in a very general context with distributed output measurements with asynchronous transmissions, which require very careful handling.

Our main contribution is the joint and systematic design of event-triggered controllers and dynamic quantizers for a general NCS setup, and we provide an approach that is feasible for any stabilizable and detectable LTI plant. To ensure that the proposed strategy is applicable in practice, the joint event-triggering and dynamic quantization design achieves the following properties:

1) an input-to-state stability (ISS) property is guaranteed for a (size-adjustable) bounded set around the origin with respect to the external disturbances and Zeno behavior is excluded. The size of the bounded set can be made arbitrarily small by selecting the tuning parameters in the design appropriately, hence, a global practical ISS property is achieved;
2) the size of the data packages that are transmitted is bounded (which is the main goal of quantization) so that at each transmission only a finite number of bits have to be communicated. This size strongly depends on the transmission instants, as we will reveal in our detailed analysis.

In addition to these two properties, we also show that:

3) at each transmission event, the output measurement is within the quantizer range;
4) the transmitted output measurement is more accurate than the information already available at the receiving node based on the last transmission instant. In conventional event-triggering setups, this is already given for free since the sampling induced error is reset to zero at each transmission instant, which is not the case in quantized event-triggered control systems and is therefore, important to handle explicitly to avoid redundant transmissions.

Despite the practical importance of the addressed problem, only a few results in the literature have investigated this topic [18]–[24]. The techniques of [18]–[21] are dedicated to the case of state feedback control. The extension of these results to the case of output feedback by modifying the triggering condition is far from trivial as Zeno behavior is likely to occur in this case, see, e.g., [7], [25], and [26]. Moreover, the results of [23] and[24] are developed for discrete-time plant models in which the triggering condition is only verified at discrete time instants (hereby, not having to consider the Zeno phenomenon) but not continuously verified as we consider in our approach. To the best of our knowledge, only [22] is applicable for the case of output feedback control of continuous-time plant model. However, [22] does not consider the presence of disturbances, which on the one hand is crucial for practical applications while on the other hand it forms a tremendous technical challenge in event-triggered control, as also highlighted in [8]. Furthermore, the practical aspects that we consider in 1–4 have not been studied in the previously mentioned works. As said, this is the first work on the design of input-to-state stabilizing event-triggered controllers with dynamic quantization of the output feedback information that deals with all the previously mentioned issues in 1–4. In addition, we handle the implementation scenario where the plant outputs are distributed and transmitted in an asynchronous fashion.

The event-triggering mechanism that we construct is inspired by [5], [25], and [27] (in which no quantization was considered). Before being sent to the controller, the sensor measurement is quantized by means of a dynamic quantizer associated to its node in order to send a finite number of bits over the digital channel. To prevent the accumulation of zoom actions, the quantizer is only allowed to update its range (and consequently its error bound) at the transmission instants of the respective node. To be more specific, the zoom in/out actions by the quantizer will be performed before the data are being sent over the network.

As already mentioned, the design procedure is feasible for any stabilizable/detectable LTI plant (and any stabilizing output-based LTI controller) and the required design steps (and to be used design conditions) are provided leading to a systematic design procedure. The solution of linear matrix inequality (LMI) is needed in order to select the tuning parameters in the event-triggered mechanism and the dynamic quantizer combination leading to the desired ISS result and size of the ISS set. Interestingly, the proposed design strategy reveals the intuitive tradeoff between the amount of transmissions and the number of quantization levels (and thereby the size of each transmitted data package). The effectiveness of the approach is illustrated on a numerical example.

A preliminary version of this study has been reported in [28]. Compared to [28], in this paper we handle a much more general scenario. Indeed, [28] only treats the case where the plant outputs are sent over a single network in a centralized fashion. Additionally, in this paper, we provide more insights on the problem and all the technical proofs are included.

II. Preliminaries

Let $\mathbb{R} := (-\infty, \infty)$, $\mathbb{R}_{\geqslant 0} := [0, \infty)$, $\mathbb{N} := \{0, 1, 2, \ldots\}$, $\mathbb{N}_{>0} := \{1, 2, \ldots\}$, and $\mathbb{Z}$ the set of integers. For a countable set S, $\text{card}(S)$ denotes its cardinality. A continuous function $\gamma : \mathbb{R}_{\geqslant 0} \to \mathbb{R}_{\geqslant 0}$ is of class $\mathcal{K}$ if it is zero at zero and strictly increasing. It is of class $\mathcal{K}_\infty$ if, in addition, $\gamma(s) \to \infty$ as $s \to \infty$. A continuous function $\gamma : \mathbb{R}^2_{\geqslant 0} \to \mathbb{R}_{\geqslant 0}$ is of class $\mathcal{KL}$ if for each fixed $t \in \mathbb{R}_{\geqslant 0}$, $\gamma(\cdot, t)$ is of class $\mathcal{K}$, and for each fixed $s \in \mathbb{R}_{\geqslant 0}$, $\gamma(s, .)$ is nonincreasing and satisfies $\lim_{t\to\infty} \gamma(s, t) = 0$. A function $V : \mathcal{X} \subset \mathbb{R}^n \to \mathbb{R}_{\geqslant 0}$ is locally Lipschitz continuous if for each $x \in \mathcal{X}$, there exists a neighborhood $\mathcal{U}_x$ and a constant $M > 0$ such that $|V(y) - V(z)| \leqslant M|y - z|$ for all $y, z \in \mathcal{U}_x$.

We denote the minimum and maximum eigenvalues of the real symmetric square matrix A as $\lambda_{\min}(A)$ and $\lambda_{\max}(A)$, respectively. We write A^T to denote the transpose of A, and $\mathbb{I}_n$ stands for the identity matrix of dimension n. For a partitioned matrix, the symbol $\star$ stands for symmetric blocks, e.g., $\left[\begin{smallmatrix} A & B \\ \star & C \end{smallmatrix}\right]$ means $\left[\begin{smallmatrix} A & B \\ B^T & C \end{smallmatrix}\right]$. We denote by $\mathbf{0}_n$ and $\mathbf{1}_n$ the vectors in $\mathbb{R}^n$ whose elements are all 0 or 1, respectively. We write $(x, y) \in \mathbb{R}^{n_x+n_y}$ to represent the vector $[x^T, y^T]^T$ for $x \in \mathbb{R}^{n_x}$ and $y \in \mathbb{R}^{n_y}$. For a vector $x \in \mathbb{R}^{n_x}$, we denote by $|x| := \sqrt{x^T x}$ its Euclidean norm and, for a matrix $A \in \mathbb{R}^{n\times m}$, $|A| := \sqrt{\lambda_{\max}(A^T A)}$. Given a set $\mathcal{A} \subset \mathbb{R}^n$ and a vector $x \in \mathbb{R}^n$, the distance of x to $\mathcal{A}$ is defined as $|x|_{\mathcal{A}} := \inf_{y\in\mathcal{A}} |x - y|$. The symbol $\wedge$ is used to represent a logical conjunction of two conditions. We use the following regularized ceiling function, for $x \in \mathbb{R}$

$$\lceil x \rceil := \begin{cases} \{\min\{k \in \mathbb{Z} : k > x\}\}, & x \notin \mathbb{Z} \\ \{x, x + 1\}, & x \in \mathbb{Z}. \end{cases} \tag{1}$$

This (set-valued) regularized ceiling function is outer semicontinuous in the sense that for each $x \in \mathbb{R}$, each sequence of points $x_i \in \mathbb{R}$ that converge to x, and each sequence of points $y_i \in \mathbb{R}$ that converge to y, $y \in \lceil x \rceil$.

We consider hybrid systems of the following form [29], [30]

$$\dot{x} \in F(x, w) \quad x \in \mathcal{C}, \quad x^+ \in G(x) \quad x \in \mathcal{D} \tag{2}$$

where $x \in \mathbb{R}^{n_x}$ is the state, $w \in \mathbb{R}^{n_w}$ is an exogenous input, $\mathcal{C}$ is the flow set, F is the flow map, $\mathcal{D}$ is the jump set, and G is the jump map. We assume that the vector field F is continuous and G is outer semicontinuous and locally bounded with respect to D, and the sets C and D are assumed to be closed, which ensures that the hybrid model (2) satisfies the basic regularity conditions, see [29, Sec. 6.2]. Solutions to system (2) are defined on hybrid time domains. We call a subset $E \subset \mathbb{R}_{\geqslant 0} \times \mathbb{N}$ a compact hybrid time domain if $E = \bigcup_{j=0}^{J-1} ([t_j, t_{j+1}], j)$ for some finite sequence of times $0 = t_0 \leqslant t_1 \leqslant \cdots \leqslant t_J$ and it is a hybrid time domain if for all $(T, J) \in E$, $E \cap ([0, T] \times \{0, 1, \cdots, J\})$ is a compact hybrid time domain. A hybrid signal is a function defined on a hybrid time domain. A hybrid signal $w : \text{dom}\, w \to \mathbb{R}^{n_w}$ is called a hybrid input if $w(\cdot, j)$ is measurable and locally essentially bounded for each j. A hybrid signal $x : \text{dom}\, x \to \mathbb{R}^{n_x}$ is called a hybrid arc if $x(\cdot, j)$ is locally absolutely continuous for each j. A hybrid arc $x : \text{dom}\, x \to \mathbb{R}^{n_x}$ and a hybrid input $w : \text{dom}\, w \to \mathbb{R}^{n_w}$ form a solution pair (x, w) to system (2) if $\text{dom}\, w = \text{dom}\, x$, $x(0, 0) \in \mathcal{C} \cup \mathcal{D}$, and:

1) for all $j \in \mathbb{N}$, and almost all t such that $(t, j) \in \text{dom}\, x$, $x(t, j) \in \mathcal{C}$ and $\dot{x}(t, j) \in F(x(t, j), w(t, j))$;
2) for all $(t, j) \in \text{dom}\, x$ such that $(t, j + 1) \in \text{dom}\, x$, $x(t, j) \in \mathcal{D}$ and $x(t, j + 1) \in G(x(t, j))$.

A solution pair (x, w) to system (2) is nontrivial if $\text{dom}\, x$ contains at least two points, maximal if it cannot be extended, it is complete if its domain, $\text{dom}\, x$, is unbounded, it is Zeno if it is complete and $\sup_t \text{dom}\, x < \infty$, where $\sup_t \text{dom}\, x := \sup\{t \in \mathbb{R}_{\geqslant 0} : \exists j \in \mathbb{N}_{>0}$ such that $(t, j) \in \text{dom}\, x\}$, and it is t-complete if $\text{dom}\, x$ is unbounded in the t-direction, i.e., $\sup_t \text{dom}\, x = \infty$.

We use the following definition of $\mathcal{L}_\infty$-norm for hybrid signals [30], [31].

Definition 1: For a hybrid signal w, with domain $\text{dom}\, w \subset \mathbb{R}_{\geqslant 0} \times \mathbb{N}$, and a scalar $T \in \mathbb{R}_{\geqslant 0}$, the T-truncated $\mathcal{L}_\infty$-norm is given by

$$\|w_{[T]}\|_\infty := \sup_{j\in\mathbb{N}} \left\{ \operatorname*{ess\,sup}_{t\in\mathbb{R}_{\geqslant 0} | (t,j)\in\text{dom}\, w,\, t+j\leqslant T} |w(t, j)| \right\}. \tag{3}$$

The $\mathcal{L}_\infty$-norm of w is given by

$$\|w\|_\infty := \lim_{T\to T^*} \|w_{[T]}\|_\infty \tag{4}$$

where $T^* := \sup\{t + j : (t, j) \in \text{dom}\, w\}$. Moreover, we say that $w \in \mathcal{L}_\infty$ whenever the above limit exists and is finite. ■

We adopt the following ISS notion for hybrid systems [30].

Definition 2: Consider the hybrid system (2), a set $\mathcal{A} \subset \mathbb{R}^{n_x}$ and a set $\mathbb{X}_0 \subseteq \mathbb{R}^{n_x}$. The set $\mathcal{A}$ is ISS w.r.t. w and initial state set $\mathbb{X}_0$ if there exist $\beta \in \mathcal{KL}$ and $\psi \in \mathcal{K}$ such that, for each $x(0, 0) \in \mathbb{X}_0$ and $w \in \mathcal{L}_\infty$, each maximal solution pair (x, w) is t-complete[1] and satisfies for all $(t, j) \in \text{dom}\, x$.

$$|x(t, j)|_{\mathcal{A}} \leqslant \max\{\beta(|x(0, 0)|_{\mathcal{A}}, t + j), \psi(||w||_\infty)\}. \tag{5}$$

■

[1]In general, t-completeness is not required in the ISS property for hybrid systems as mentioned in [30, Remark 2.2]. However, in the context of NCSs, it is desired that all solutions are t-complete and is therefore explicitly required in this definition.

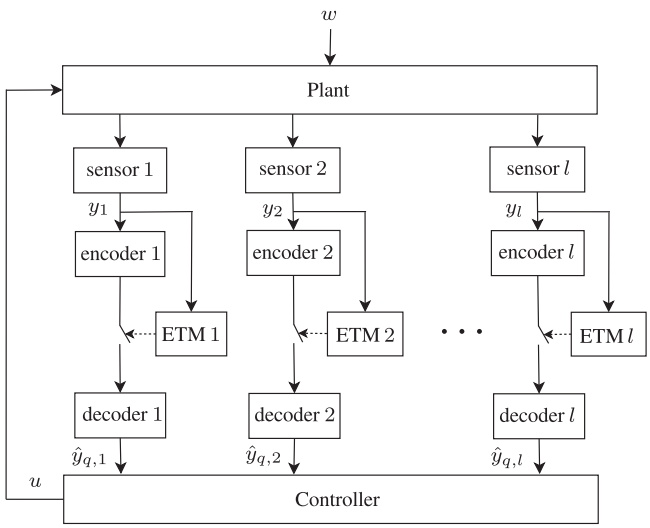

Fig. 1. NCS with distributed and quantized output measurements.

III. Problem Formulation

Consider the continuous-time plant model

$$\dot{x}_p = A_p x_p + B_p u + E_p w, \qquad y = C_p x_p \tag{6}$$

where $x_p \in \mathbb{R}^{n_p}$ is the plant state, $u \in \mathbb{R}^{n_u}$ is the control input, $w \in \mathbb{R}^{n_w}$ is unknown plant disturbance, and $y \in \mathbb{R}^{n_y}$ is the measured output. The disturbance w is assumed to be Lebesgue measurable and locally bounded. The plant is stabilized by a dynamic controller of the form

$$\dot{x}_c = A_c x_c + B_c \hat{y}_q, \qquad u = C_c x_c + D_c \hat{y}_q \tag{7}$$

where $x_c \in \mathbb{R}^{n_c}$ is the controller state and $\hat{y}_q \in \mathbb{R}^{n_y}$ denotes the most recent quantized output measurement available at the controller, see Fig. 1. The controller (7) is designed by an emulation approach in the sense that we assume that the closed-loop system given by (6) and (7) is stable when the effects of both the quantization and the network are absent, i.e., when $\hat{y}_q = y$.

A. Setup Description

We consider the scenario where the controller is directly connected to the plant while the output measurement is transmitted to the controller over a digital channel. This control architecture has many practical applications in control systems based on (wireless) sensor networks such as in heat, ventilation, and air-conditioning control systems [32] and in vehicle platoons [3, Ch. 3]. In particular, we assume that the plant has l distributed output measurements $y_1, y_2, \ldots, y_l$, which are measured by l distributed sensors. The sensors communicate with the controller at discrete time instants t_k^i, $k \in \mathbb{N}, i \in \{1, 2, \ldots, l\}$. At any node $i \in \{1, 2, \ldots, l\}$, the measured output $y_i \in \mathbb{R}^{n_{y_i}}$ is collected, quantized, encoded, and the resulting encrypted data is sent over the communication channel, see Fig. 1. This encryption is required to make sure that at each transmission, only a limited number of bits is sent.

Let $\hat{y}_q = (\hat{y}_{q,1}, \hat{y}_{q,2}, \ldots, \hat{y}_{q,l})$, where $\hat{y}_{q,i}$, $i \in \{1, 2, \ldots, l\}$, denote the most recent quantized value of y_i available at the controller. The value of $\hat{y}_{q,i}$ is kept constant between two consecutive transmission instants of node i in a zero-order-hold (ZOH) fashion, i.e., $\dot{\hat{y}}_{q,i} = 0$. We ignore communication and computation delays in this study, although it would be possible to include them by using the techniques in, e.g., [2], [25].

B. Event-Triggering Mechanism

The sequence of transmission instants of each node i is generated by an independent event-triggering condition in the sense that the event-triggering condition depends only on locally available information at node i. Each triggering mechanism determines the next transmission instant t_k^i, $k \in \mathbb{N}, i \in \{1, 2, \ldots, l\}$ based on the actual values of the output measurement y_i of node i and the most recent transmitted (quantized) value $\hat{y}_{q,i}$. The triggering mechanism at each node $i \in \{1, 2, \ldots, l\}$ is dynamic in the sense of [5], [25], and [27] and takes the following form:

$$t_{k+1}^i = \inf\{t > t_k^i + T_i \mid \eta_i(t) = 0\} \tag{8}$$

where $t_0^i = 0, T_i > 0$ and $\eta_i : \mathbb{R}_{\geqslant 0} \to \mathbb{R}_{\geqslant 0}$. The time constant $T_i > 0, i \in \{1, 2, \ldots, l\}$ is a strictly positive lower bound on the intertransmission times of the output y_i that we enforce to prevent the occurrence of Zeno with respect to transmission events at node i. The variable $\eta_i, i \in \{1, 2, \ldots, l\}$, is the solution to the dynamical system

$$\dot{\eta}_i \in \Psi_i(o_i) \quad t \in (t_k^i, t_{k+1}^i), \qquad \eta_i((t_k^i)^+) = \eta_{0,i}(o_i) \tag{9}$$

where $o_i \in \mathbb{R}^{n_{o_i}}$ represents locally available information at the event-triggering mechanism. The time constant T_i and the functions Ψ_i and $\eta_{0,i}$ are to be designed and will be specified in Section V.

C. Dynamic Quantization

As mentioned earlier, at each transmission instant t_k^i, $k \in \mathbb{N}, i \in \{1, 2, \ldots, l\}$, the value of y_i is quantized before being sent over the network. A quantizer is essentially a piecewise constant function $q_i : \mathbb{R}^{n_{y_i}} \to Q_i \subseteq \mathbb{R}^{n_{y_i}}$ with Q_i a finite subset of $\mathbb{R}^{n_{y_i}}$. As such, a quantizer induces a partition in $\mathbb{R}^{n_{y_i}}$ consisting of $\text{card}(Q_i)$ quantization regions described by $\{z \in \mathbb{R}^{n_{y_i}} : q_i(z) = x\}$, $x \in Q_i$. We assume that the function q_i satisfies the following assumption as proposed in [33], see also [9], [10], [16].

Assumption 1: [33] There exist constants M_i, Δ_i, $i \in \{1, 2, \ldots, l\}$, such that for all $y_i \in \mathbb{R}^{n_{y_i}}$, it holds that

$$|y_i| \leqslant M_i \Rightarrow \ |q_i(y_i) - y_i| \leqslant \Delta_i. \tag{10}$$

Moreover, there exists a constant $\delta > 0$ such that for all $z \in \mathbb{R}^{n_{y_i}}$ with $|z| \leqslant \delta$, it holds that $q(z) = 0$. ■

This assumption in essence states that the magnitude of the quantization error $|q_i(y_i) - y_i|$ is upper bounded by Δ_i, as long as the quantizer is not saturated, i.e., the output measurement y_i is within the range of its respective quantizer. Moreover, it states that $q_i(z) = 0$ for z in some neighborhood around the origin (and implies $0 \in Q_i$). Let us remark that Assumption 1 allows the quantizer regions to have arbitrary shapes. In the remainder of the paper, we will refer to M_i and Δ_i as the initial

quantizer range and initial error bound of node $i \in \{1, 2, \ldots, l\}$, respectively.

In this paper, we consider dynamic quantizer functions $q_i^{\mu_i}$, $i \in \{1, 2, \ldots, l\}$, which, as in [15], [16], and [33] are defined as

$$q_i^{\mu_i}(y_i) := \mu_i q_i\left(\frac{y_i}{\mu_i}\right) \tag{11}$$

where $\mu_i \in \mathbb{R}_{\geqslant \underline{\mu}_i}$, $i \in \{1, 2, \ldots, l\}$, are dynamic variables referred to as the zoom variables and where q_i satisfies Assumption 1 for some $M_i, \Delta_i > 0$ and where $\underline{\mu}_i > 0$ is a lower-bound on μ_i to be specified. The zoom variables μ_i, $i \in \{1, 2, \ldots, l\}$, are used to adjust the quantizer range initially equal to $M_i > 0$ and the quantizer error bound initially equal to $\Delta_i > 0$ of node i based on the magnitude of the output measurement y_i. To be more specific, the range and the error bound of the dynamic quantizer as in (11) are given by $M_i\mu_i$ and $\Delta_i\mu_i$, respectively. As such, property (10) becomes $|y_i| \leqslant \mu_i M_i \quad \Rightarrow |q_i^{\mu_i}(y_i) - y_i| \leqslant \mu_i \Delta_i$. The number of quantization regions of dynamic quantizers remains constant all the time.

In the context of NCSs, it is of importance that at each transmission instant, before data are actually transmitted, the dynamic quantizer is set such that property 3 and 4 mentioned in Section I are satisfied. To achieve these two properties, the zoom variable μ_i is adapted at transmission instants $t_k^i, k \in \mathbb{N}$, $i \in \{1, 2, \ldots, l\}$, according to

$$\mu_i^+ \in \Theta_i(y_i, \mu_i) := \Omega_{\text{in},i}^{\kappa_{\text{in},i}(y_i,\mu_i)} \Omega_{\text{out},i}^{\kappa_{\text{out},i}(y_i,\mu_i)} \mu_i \tag{12}$$

where $\Omega_{\text{in},i} \in (0, 1), \Omega_{\text{out},i} > 1$, are the zoom-in and zoom-out factors, respectively, and where we omitted the time arguments for the sake of compactness. The functions $\kappa_{\text{in},i}, \kappa_{\text{out},i} : \mathbb{R}^{n_{y_i}} \times \mathbb{R}_{>0} \rightrightarrows \mathbb{N}$ determine the number of zoom-in or zoom-out actions that need to be performed at each transmission.[2]

Let us elaborate on the dynamic adjustment strategy of μ_i, $i \in \{1, 2, \ldots, l\}$. At any transmission instant t_k^i, $k \in \mathbb{N}, i \in \{1, 2, \ldots, l\}$, if the magnitude of $|y_i|$ is close to the range of the quantizer, we increase the value of μ_i with the factor $\sigma_{\text{out},i} \in \Omega_{\text{out},i}^{\kappa_{\text{out},i}(y_i,\mu_i)}$ with $\sigma_{\text{out},i} > 1$ in order to make sure that the transmitted information is within range of the quantizer (which corresponds to property 3 stated in Section I). We refer to this action as the zoom-out event. On the other hand, if $|y_i|$ is small with respect to the current quantizer error bound, we decrease μ_i by means of the zoom-in factor $\sigma_{\text{in},i} \in \Omega_{\text{in},i}^{\kappa_{\text{in},i}(y_i,\mu_i)}$ with $\sigma_{\text{in},i} \in (0, 1)$ such that more precise information is transmitted (which corresponds to property 4 stated in Section I). We refer to this action as the zoom-in event. See, e.g., [16] for more details on dynamic quantizers.

Let us emphasize that the zoom variable μ_i in (12) is only updated at transmission instants t_k^i, $k \in \mathbb{N}, i \in \{1, 2, \ldots, l\}$ and held constant in between transmissions, i.e., $\dot{\mu}_i = 0$ for $t \in (t_k^i, t_{k+1}^i)$. Consequently, in each node $i \in \{1, 2, \ldots, l\}$, the time in between the zoom events is lower bounded by the minimum intertransmission time T_i ensured by the local triggering condition (8).

[2] In (12), we use $\Omega_{\text{in},i}^{\kappa_{\text{in},i}(y_i,\mu_i)}$ to denote the set $\{\Omega_{\text{in},i}^{\kappa} \mid \kappa \in \kappa_{\text{in},i}(y_i, \mu_i)\}$ and $\Omega_{\text{out},i}^{\kappa_{\text{out},i}(y_i,\mu_i)}$ to denote the set $\{\Omega_{\text{out},i}^{\kappa} \mid \kappa \in \kappa_{\text{out},i}(y_i, \mu_i)\}$.

To be able to successfully reconstruct the broadcast encoded information, the zoom variable μ_i of both the encoder and the decoder at any channel should be initialized at the same value and the quantization regions Q_i and the zoom factor Ω_{in} and Ω_{out} should be known at both the encoder and decoder, see [34], [35], and [10, Remark 1] for an in-depth discussion on this point. Then, at each update instant t_k^i, we only transmit the index of the quantization region, the number of required zoom actions corresponding to the transmission, and a boolean (one bit) that indicates whether these zoom actions are zoom-in or zoom-out events. By means of these three (two integers and one boolean) quantities, the decoder on the other side of the network can update μ_i according to (12) and thereby the quantized output $\hat{y}_{q,i}$ using (11), which then can be used by the controller according to (7).

D. Problem Statement

Our objective is to design both the event-triggering mechanism (8), (9) (i.e., to design the time constant T_i and the functions Ψ_i and $\eta_{0,i}$ for $i \in \{1, 2, \ldots, l\}$) and the dynamic quantization strategy (12) (i.e., to design the parameters $\Delta_i, M_i, \Omega_{\text{in},i}, \Omega_{\text{out},i}$ and the functions $\kappa_{\text{in},i}, \kappa_{\text{out},i}$ for $i \in \{1, 2, \ldots, l\}$) such that properties 1–4 mentioned in Section I are achieved for the closed-loop system.

IV. Hybrid Model

In this section, we present a formal description of the closed-loop system using the modeling framework for hybrid dynamical systems as advocated in [29], see, e.g., [36] and [29, e.g., 1.5] for the modeling of quantized control systems in the hybrid formalism. We define the network-induced error as $e_{s,i} := \hat{y}_{q,i} - q_i^{\mu_i}(y_i)$, which is reset to zero at each transmission instant $t_k^i, k \in \mathbb{N}$. We also define the quantization error as $e_{q,i} := q_i^{\mu_i}(y_i) - y_i$. The total network-induced error at each node $i \in \{1, 2, \ldots, l\}$ is given by

$$e_i := e_{s,i} + e_{q,i} = \hat{y}_{q,i} - y_i. \tag{13}$$

Since at each transmission instant t_k^i, $k \in \mathbb{N}, i \in \{1, 2, \ldots, l\}$, the sampling error of node i is set to zero, we have that

$$e_i(t_k^{i\,+}) = e_{q,i}(t_k^{i\,+}). \tag{14}$$

Observe that in general e_i is not reset to zero at each transmission instant due to the effect of quantization. This issue induces nontrivial challenges to the design of event-triggered control mechanisms, compared to the case where quantization is not considered, and requires careful handling. In fact, this phenomenon may have a negative impact on the closed-loop stability, as we will explain later. Let $x := (x_p, x_c) \in \mathbb{R}^{n_x}$ and $e := (e_1, e_2, \ldots, e_l) \in \mathbb{R}^{n_y}$. Then, in view of (6), (7), and (13), the flow dynamics of x is given by

$$\dot{x} = \mathcal{A}_1 x + \mathcal{B}_1 e + \mathcal{E}_1 w \tag{15}$$

where $\mathcal{A}_1 := \left[\begin{smallmatrix} A_p + B_p D_c C_p & B_p C_c \\ B_c C_p & A_c \end{smallmatrix}\right]$, $\mathcal{B}_1 := \left[\begin{smallmatrix} B_p D_c \\ B_c \end{smallmatrix}\right]$, and $\mathcal{E}_1 := \left[\begin{smallmatrix} E_p \\ 0 \end{smallmatrix}\right]$. Let the matrix C_p in (6) be partitioned as $C_p = [C_{p,1}^T \ \ldots \ C_{p,l}^T]^T$ with $C_{p,i} \in \mathbb{R}^{n_{y_i}} \times \mathbb{R}^{n_p}$ such that $y_i = C_{p,i} x_p \in$

$\mathbb{R}^{n_{y_i}}$ for $i \in \{1, 2, \ldots, l\}$. Then, because of the ZOH implementation, the flow dynamics of e_i is

$$\dot{e}_i = -\dot{y}_i = -C_{p,i}\dot{x}_p = \mathcal{A}_{2i}x + \mathcal{B}_{2i}e + \mathcal{E}_{2i}w \tag{16}$$

where $\mathcal{A}_{2i} := \left[\begin{smallmatrix} -C_{p,i}(A_p + B_p D_c C_p) \\ -C_{p,i}B_p C_c \end{smallmatrix}\right]$, $\mathcal{B}_{2i} := [\, -C_{p,i}B_p D_c \,]$, and $\mathcal{E}_{2i} := [\, -C_{p,i}E_p \,]$. In view of (16), the flow dynamics of the overall e is

$$\dot{e} = \mathcal{A}_2 x + \mathcal{B}_2 e + \mathcal{E}_2 w \tag{17}$$

where

$$\mathcal{A}_2 := \begin{bmatrix} \mathcal{A}_{21} \\ \vdots \\ \mathcal{A}_{2l} \end{bmatrix}, \mathcal{B}_2 := \begin{bmatrix} \mathcal{B}_{21} \\ \vdots \\ \mathcal{B}_{2l} \end{bmatrix}, \text{ and } \mathcal{E}_2 := \begin{bmatrix} \mathcal{E}_{21} \\ \vdots \\ \mathcal{E}_{2l} \end{bmatrix}.$$

We introduce auxiliary variables $\tau_i \in \mathbb{R}_{\geqslant 0}$ and $p_i \in \{0, 1\}$ for $i \in \{1, 2, \ldots, l\}$. The variable τ_i represents the time elapsed since the last transmission instant of node i. It has the dynamics

$$\dot{\tau}_i = 1 \quad t \in (t_k^i, t_{k+1}^i), \quad \tau_i((t_k^i)^+) = 0 \quad \text{for } k \in \mathbb{N}. \tag{18}$$

The variable p_i is a boolean that keeps track of whether at the next event, the zoom variable is updated ($p_i = 0$) or a transmission occurs ($p_i = 1$) (recall that at each transmission instant t_k^i, the zoom variable μ_i is updated before y_i is transmitted). Let $\xi := (x, e, \mu, \tau, \eta, p) \in \mathbb{X}$ with $\mathbb{X} = \mathbb{R}^{n_x} \times \mathbb{R}^{n_y} \times (\mathbb{R}_{\geqslant \underline{\mu}_1} \times \ldots \times \mathbb{R}_{\geqslant \underline{\mu}_l}) \times \mathbb{R}^l_{\geqslant 0} \times \mathbb{R}^l_{\geqslant 0} \times \{0, 1\}^l$ be the concatenation of the state variables, where $\mu := (\mu_1, \ldots, \mu_l) \in \mathbb{R}_{\geqslant 0} \times \ldots \times \mathbb{R}_{\geqslant 0}$, $\tau := (\tau_1, \ldots, \tau_l) \in \mathbb{R}^l_{\geqslant 0}$, $\eta := (\eta_1, \ldots, \eta_l) \in \mathbb{R}^l_{\geqslant 0}$, and $p := (p_1, \ldots, p_l) \in \{0, 1\}^l$. Then, in view of (8) and (9), the flow set $\mathcal{C}$ and the jump set $\mathcal{D}$ are given by

$$\mathcal{C} := \Big\{\xi \in \mathbb{X} : p = 0\Big\}, \qquad \mathcal{D} := \bigcup_{i=1}^{l} \mathcal{D}_i \tag{19}$$

with $\mathcal{D}_i := \{\xi \in \mathbb{X} : (\eta_i = 0 \text{ and } \tau_i \geqslant T_i) \text{ or } p_i = 1\}$. The triggering condition related to $\eta_i(t) = 0$, $i \in \{1, 2, \ldots, l\}$, in (8) is embedded in the flow set $\mathcal{C}$ via the definition of $\mathbb{X}$ ($\xi \in \mathbb{X}$ implies $\eta_i \geqslant 0$ for each $i \in \{1, 2, \ldots, l\}$). Given (19), we obtain the hybrid system[3]

$$\begin{aligned} \dot{\xi} \in F(\xi, w) := \left\{ \begin{pmatrix} \mathcal{A}_1 x + \mathcal{B}_1 e + \mathcal{E}_1 w \\ \mathcal{A}_2 x + \mathcal{B}_2 e + \mathcal{E}_2 w \\ \mathbf{0}_l \\ \mathbf{1}_l \\ \Psi(o) \\ \mathbf{0}_l \end{pmatrix} \right\} \quad & \xi \in \mathcal{C} \\ \xi^+ \in G(\xi) \quad & \xi \in \mathcal{D} \end{aligned} \tag{20}$$

where $\Psi(o) := (\Psi_1(o_1), \ldots, \Psi_l(o_l))$ with $o_i := (y_i, e_i, \tau_i, \eta_i) \in \mathbb{R}^{n_{o_i}}$. In view of the update conditions of η_i in (9), μ_i in (12), e_i after (13), τ_i in (18), and p_i after (18), the jump map is given by $G(\xi) := \bigcup_{i=1}^{l} G_i(\xi)$, where

$$G_i(\xi) := \begin{cases} \left\{G_i^{\mu}(\xi)\right\} & \text{for } \xi \in \mathcal{D}_i \wedge p_i = 0 \\ \left\{G_i^{y}(\xi)\right\} & \text{for } \xi \in \mathcal{D}_i \wedge p_i = 1 \\ \emptyset & \text{for } \xi \notin \mathcal{D}_i \end{cases} \tag{21}$$

with

$$G_i^{\mu}(\xi) := \begin{pmatrix} x \\ e \\ \bar{\Lambda}_i \Theta_i(y_i, \mu_i) + (\mathbb{I}_l - \bar{\Lambda}_i)\mu \\ \tau \\ \eta \\ \bar{\Lambda}_i \mathbf{1}_l + (\mathbb{I}_l - \bar{\Lambda}_i)p \end{pmatrix}$$

$$G_i^{y}(\xi) := \begin{pmatrix} x \\ \Lambda_i e_q + (\mathbb{I}_{n_y} - \Lambda_i)e \\ \mu \\ (\mathbb{I}_l - \bar{\Lambda}_i)\tau \\ \bar{\Lambda}_i \eta_0(e) + (\mathbb{I}_l - \bar{\Lambda}_i)\eta \\ (\mathbb{I}_l - \bar{\Lambda}_i)p \end{pmatrix} \tag{22}$$

where $\Lambda_i := \text{diag}\{\delta_{1i}\mathbb{I}_{n_{y1}}, \ldots, \delta_{li}\mathbb{I}_{n_{yl}}\}$, $i \in \{1, 2, \ldots, l\}$, $\bar{\Lambda}_i := \text{diag}\{\delta_{1i}, \ldots, \delta_{li}\}$ with δ_{ji} the Kronecker delta, which takes the value $\delta_{ji} = 1$ when $i = j$ and $\delta_{ji} = 0$ when $i \neq j$, $\eta_0(e) := (\eta_{0,1}(e_1), \ldots, \eta_{0,l}(e_l))$, $e_q := (e_{q,1}, \ldots, e_{q,l})$, the function $\Theta_i : \mathbb{R}^{n_{y_i}} \times \mathbb{R}_{\geqslant 0} \rightrightarrows \mathbb{R}_{\geqslant 0}$ as in (12) with the functions $\kappa_{\text{in},i}, \kappa_{\text{out},i} : \mathbb{R}^{n_{y_i}} \times \mathbb{R}_{\geqslant 0} \rightrightarrows \mathbb{N}$ to be specified.

System (20) flows on $\mathcal{C}$ as long as the triggering conditions are not satisfied and $p = 0$. When $\xi \in \mathcal{D}_i$ and $p_i = 0$, ξ can jump according to $\xi^+ \in G_i^{\mu}(\xi)$ corresponding to an update of the quantizer settings. To be more specific, when the state jumps according to $\xi^+ \in G_i^{\mu}(\xi)$, the quantizer variable μ_i, $i \in \{1, 2, \ldots, l\}$, is updated and p_i is changed to one. Consequently, ξ^+ lies into the jump set $\mathcal{D}_i$ with $p_i = 1$. Since the system is not allowed to flow when $p_i = 1$ for some $i \in \{1, 2, \ldots, l\}$, since, in view of (19), $\xi \notin \mathcal{C}$ when $p_i = 1$ for some $i \in \{1, 2, \ldots, l\}$, a transmission is generated and p_i is reset to zero, in view of the jump map $G_i^{y}(\xi)$. As such, the boolean variable p_i ensures that at any transmission instant t_k^i, the quantizer variable μ_i is updated before transmitting $q_i^{\mu_i}(y_i)$, which is fundamental for realizing properties 2 and 3 as mentioned in the introduction.

Let us remark that the hybrid system in (20) satisfies the following conditions:

1) $\mathcal{C}$ and $\mathcal{D}$ are closed sets;
2) $F : \mathbb{X} \times \mathbb{R}^{n_w} \rightrightarrows \mathbb{X}$ is outer semicontinuous and locally bounded, and $F(\xi, w)$ is nonempty and convex for all $(\xi, w) \in \mathcal{C} \times \mathbb{R}^{n_w}$;
3) $G : \mathbb{X} \rightrightarrows \mathbb{X}$ is outer semicontinuous and locally bounded, and $G(\xi, w)$ is nonempty for all $(\xi, w) \in \mathcal{D}$.

These conditions assure that the hybrid system $\mathcal{H}$ described by (19) and (20), is well posed, see also, [29, Ch. 6].

Remark 1: We note that the dynamic quantization strategy in (12), (20), and (22) involves some differences compared to related techniques in the context of quantized control systems (QCS) [16], [36], [39]. First, in the proposed scheme, the zoom

[3]With no loss of generality, we assume that before the first hybrid time instant, i.e., $(t, j) = (0, 0)$, the system is properly initialized in the sense that at least one successful transmission per node has occurred. The latter is important to make sure that both the sensors and the controller have the same knowledge on $\hat{y}_q$ at the initial time. This prevents the system to start in an undesired equilibrium due to the mismatch between the controller and the sensor on the last transmitted value $\hat{y}_q$, see also, e.g., [7], [37], [38].

actions are carried out based on the past (true) values of y_i and not based on the quantized feedback information $q_i^{\mu_i}(y_i)$ as in [16], [36], [39] for instance. To that end, we rely on the assumption that the true values of y_i can be accessed by the corresponding encoder at node i. Indeed, this requirement is relevant if the communication network is the reason of quantization, such as in e.g., [22], [40]–[42] and as we consider in this study, but not the sensor, see [39] for further discussion on this point. Second, unlike [16], [39], we do not reset the control input to zero during a zoom-out event, which allows to avoid large overshoots during the zoom-out event. ■

V. Main Result

A. Design Conditions for the Event-Triggering Mechanism

We make the following design condition regarding system (20) to construct the event-triggering mechanism appropriately. This is always feasible for any plant–controller combination (6), (7), which in the absence of the network ($e = 0$) and disturbances ($w = 0$) is asymptotically stable (i.e., $\mathcal{A}_1$ is Hurwitz). Clearly, the design of such a controller is always possible if the plant (6) is stabilizable and detectable.

Condition 1: Consider system (20). There exist a positive definite symmetric real matrix P, real numbers $\varepsilon_x, \varepsilon_w > 0$ and $\varepsilon_{y_i}, \gamma_i > 0$ for $i \in \{1, 2, \ldots, l\}$, such that

$$\begin{pmatrix} \Sigma & \star & \star \\ \mathcal{B}_1^T P + \overline{\mathcal{B}}_2^T \mathcal{A}_2 & -\Gamma^2 + \overline{\mathcal{B}}_2^T \overline{\mathcal{B}}_2 & \star \\ \mathcal{E}_1^T P + \mathcal{E}_2^T \mathcal{A}_2 & \mathcal{E}_2^T \overline{\mathcal{B}}_2 & \mathcal{E}_2^T \mathcal{E}_2 - \varepsilon_w \mathbb{I}_{n_w} \end{pmatrix} \leqslant 0 \quad (23)$$

where $\Sigma := \mathcal{A}_1^T P + P\mathcal{A}_1 + \varepsilon_x \mathbb{I}_{n_x} + \mathcal{A}_2^T \mathcal{A}_2 + \overline{C}_p^T \Upsilon \overline{C}_p$, $\overline{C}_p := [C_p \ \ 0]$, with $\Upsilon := \operatorname{diag}\{\varepsilon_{y_1} \mathbb{I}_{n_{y_1}}, \ldots, \varepsilon_{y_l} \mathbb{I}_{n_{y_l}}\}$, $\Gamma := \operatorname{diag}\{\gamma_1 \mathbb{I}_{n_{y_1}}, \ldots, \gamma_l \mathbb{I}_{n_{y_l}}\}$, and $\overline{\mathcal{B}}_2 = [\overline{\mathcal{B}}_{21}^T \ \cdots \ \overline{\mathcal{B}}_{2l}^T]^T$ with $\overline{\mathcal{B}}_{2i} := \mathcal{B}_{2i}(\mathbb{I}_{n_y} - \Lambda_i)$. ■

The LMI condition (23) in essence establishes an $\mathcal{L}_2$-gain stability property for the system $\dot{x} = \mathcal{A}_1 x + \mathcal{B}_1 e + \mathcal{E}_1 w$ from (e, w) to $(\mathcal{A}_2 x + \overline{\mathcal{B}}_2 e + \mathcal{E}_2 w, y)$. Indeed, if we define $V(x) := x^T P x$ for all $x \in \mathbb{R}^{n_x}$, then in view of (20) and the definitions of $\Upsilon, \Gamma, \Lambda$, the feasibility of (23) is equivalent to, for all $(x, e, w) \in \mathbb{R}^{n_x + n_e + n_w}$

$$\langle \nabla V(x), \mathcal{A}_1 x + \mathcal{B}_1 e + \mathcal{E}_1 w \rangle \leqslant -\varepsilon_x |x|^2 - \sum_{i=1}^{l} \varepsilon_{y_i} |y_i|^2$$

$$- \sum_{i=1}^{l} \left| \mathcal{A}_{2i} x + \overline{\mathcal{B}}_{2i} e + \mathcal{E}_{2i} w \right|^2 + \sum_{i=1}^{l} \gamma_i^2 |e_i|^2 + \varepsilon_w |w|^2. \quad (24)$$

This property is needed to design the enforced minimum time $T_i, i \in \{1, 2, \ldots, l\}$, on the intertransmission times of each node and to design the dynamics of $\eta_i, i \in \{1, 2, \ldots, l\}$, in (19) such that closed-loop stability (in an appropriate sense) is guaranteed.

As already shortly indicated earlier, inequality (24) can always be satisfied if the matrix $\mathcal{A}_1$ is Hurwitz, i.e., if the closed-loop system (6), (7) is stable in the absence of the communication network, by selecting the matrix P and the parameters γ_i, ε_w sufficiently large. As a consequence, since LMI (23) is equivalent to inequality (24), we deduce that LMI (23) can be made feasible for any stabilizable and detectable plant model (6) by taking any arbitrary stabilizing controller (7). Furthermore, since the required conditions are in essence Lyapunov-based conditions, this will be helpful in extending the application of our technique on nonlinear systems, which is another advantage of the approach.

To sum up, we first formulate the closed-loop system in the hybrid framework (20) and then we solve LMI (23). By doing so, we obtain the matrix P and the parameters $\varepsilon_x, \varepsilon_w > 0$ and $\varepsilon_{y_i}, \gamma_i > 0$ for $i \in \{1, 2, \ldots, l\}$, which are needed to design the event-triggering mechanism and the enforced lower bound on the intertransmission times, as explained in the next section.

The dynamics of the functions $\eta_i, i \in \{1, 2, \ldots, l\}$, in (9) are defined by the functions Ψ_i and $\eta_{0,i}$, inspired by [25], where quantization was not considered, and are given by[4]

$$\Psi_i(o_i) := \varepsilon_{y_i} \max\left\{|y_i|^2, \Delta_{0,i}^2\right\} - (1 - \omega_i(\tau_i))\tilde{\gamma}_i |e_i|^2 - \vartheta_i \eta_i$$

$$\eta_{0,i}(e_i) := \gamma_i(\tilde{\lambda}_i - \lambda_i)|e_i|^2 \quad (25)$$

where

$$\omega_i(\tau_i) := \begin{cases} \{1\}, & \text{for } \tau_i \in [0, T_i) \\ [0, 1], & \text{for } \tau_i = T_i \\ \{0\}, & \text{for } \tau_i > T_i \end{cases} \quad (26)$$

and where $o_i = (y_i, e_i, \tau_i, \eta_i)$ as before, and the constants ε_{y_i}, γ_i as in Condition 1. The constants $\Delta_{0,i} > 0$ and $\vartheta_i > 0$ can be arbitrarily chosen (sufficiently small). The parameter $\tilde{\gamma}_i$ is given by $\tilde{\gamma}_i := \gamma_i^2 + \gamma_i^2 \tilde{\lambda}_i^2 + 2\gamma_i \tilde{\lambda}_i \tilde{L}_i$ with $\lambda_i \in (0, 1)$, $\tilde{\lambda}_i \in [\lambda_i, \lambda_i^{-1})$, $\tilde{L}_i := L_i + \nu_i$ for any $\nu_i > 0$ sufficiently small and $L_i := |\mathcal{B}_{2i}\Lambda_i| = |b_{2i,i}|$, with $b_{2i,i}$ such that $\mathcal{B}_{2i} = \begin{bmatrix} b_{2i,1} & \ldots & b_{2i,l} \end{bmatrix}$. The constants $\Delta_{0,i} > 0, \vartheta_i > 0, \nu_i > 0$ can be tuned to adjust the upper bound on the size of the set around the origin for which the ISS property is guaranteed, as shown in Section V-C. The time constant T_i of any node $i \in \{1, 2, \ldots, l\}$ is taken such that $T_i = \mathcal{T}_i(\lambda_i, \tilde{\lambda}_i, \gamma_i, \tilde{L}_i)$, where

$$\mathcal{T}_i(\lambda_i, \tilde{\lambda}_i, \gamma_i, \tilde{L}_i) := \begin{cases} \frac{1}{\tilde{L}_i r_i} \arctan\left(\frac{r_i(1 - \lambda_i \tilde{\lambda}_i)}{\frac{\gamma_i}{\tilde{L}_i}(\lambda_i + \tilde{\lambda}_i) + 1 + \lambda_i \tilde{\lambda}_i}\right), & \gamma_i > \tilde{L}_i \\ \frac{1}{\tilde{L}_i} \frac{1 - \lambda_i \tilde{\lambda}_i}{\lambda_i \tilde{\lambda}_i + \lambda_i + \tilde{\lambda}_i + 1}, & \gamma_i = \tilde{L}_i \\ \frac{1}{\tilde{L}_i r_i} \operatorname{arctanh}\left(\frac{r_i(1 - \lambda_i \tilde{\lambda}_i)}{\frac{\gamma_i}{\tilde{L}_i}(\lambda_i + \tilde{\lambda}_i) + 1 + \lambda_i \tilde{\lambda}_i}\right), & \gamma_i < \tilde{L}_i \end{cases} \quad (27)$$

with $r_i := \sqrt{|(\frac{\gamma_i}{\tilde{L}_i})^2 - 1|}$. When $\tilde{\lambda}_i = \lambda_i$, the time $\mathcal{T}_i(\lambda_i, \tilde{\lambda}_i, \gamma_i, \tilde{L}_i)$ corresponds to the maximally allowable transmission interval (MATI) of time-triggered controllers [43] for NCSs without quantization. Let us remark that λ_i also has an important role in the design of the quantizer, as we will discuss later in Section V-D. The time constant T_i as given in (27) is derived as the time it takes for the function $\phi_i : \mathbb{R}_{\geqslant 0} \to \mathbb{R}_{\geqslant 0}$ to decrease from

[4] In (25), we use $\varepsilon_{y_i} \max\left\{|y_i|^2, \Delta_{0,i}^2\right\} - (1 - \omega_i(\tau_i))\tilde{\gamma}_i |e_i|^2 - \vartheta_i \eta_i$ to denote the set $\{\varepsilon_{y_i} \max\left\{|y_i|^2, \Delta_{0,i}^2\right\} - (1 - \omega)\tilde{\gamma}_i |e_i|^2 - \vartheta_i \eta_i \mid \omega \in \omega_i(\tau_i)\}$.

$\phi_i(0) = \lambda_i^{-1}$ to $\phi_i(T_i) = \tilde{\lambda}_i$, where ϕ_i satisfies, see also [25], [43]

$$\frac{d\phi_i}{d\tau_i} = -2\tilde{L}_i\phi_i(\tau_i) - \gamma_i(\phi_i^2(\tau_i) + 1). \tag{28}$$

The flow and jump dynamics of the variables η_i, ϕ_i involve important differences compared to those defined in [25] to cope with the quantization effect.

Remark 2: We observe that, in view of (27) and its interpretation in terms of (28), when $\tilde{\lambda}_i \in [\lambda_i, \lambda_i^{-1})$ is increased, the guaranteed minimum time T_i between two transmission instants of node i will be reduced. However, by increasing $\tilde{\lambda}_i$, the value of $\eta_{0,i}$ in (25) will increase. Consequently, this may lead to an increase in the time it takes for η_i to decrease to zero, i.e., it may enlarge the intertransmission times. Hence, the tuning of $\tilde{\lambda}_i$ may generate a tradeoff between the guaranteed minimum intertransmission time T_i and the average intertransmission times. ■

B. Design Conditions for the Dynamic Quantizer

In this section, we specify how to design the parameters $\Delta_i, M_i, \Omega_{\text{in},i}, \Omega_{\text{out},i}$ and the functions $\kappa_{\text{in},i}, \kappa_{\text{out},i}$ for $i \in \{1, 2, \ldots, l\}$, see (12). For each node $i \in \{1, 2, \ldots, l\}$, we design the initial quantizer range M_i, the initial error bound Δ_i, the zoom-in parameters $\Omega_{\text{in},i} \in (0, 1)$, and the zoom-out parameters $\Omega_{\text{out},i} > 1$ such that

$$\frac{M_i}{\Delta_i} \geqslant \left(\kappa_i + \frac{2\sqrt{\tilde{\gamma}_i}}{\sqrt{\varepsilon_{y_i}}\Omega_{\text{in},i}\lambda_i}\right) \tag{29}$$

$$\kappa_i > \max\left\{1, \frac{(\Omega_{\text{in},i}\Omega_{\text{out},i} - 1)M_i + \Delta_i}{\Omega_{\text{in},i}\Omega_{\text{out},i}\Delta_i}\right\}. \tag{30}$$

Moreover, the functions $\kappa_{\text{in},i}$ and $\kappa_{\text{out},i}$ for $i \in \{1, 2, \ldots, l\}$, are, for $y_i \in \mathbb{R}^{n_{y_i}}$ and $\mu_i \in \mathbb{R}_{\geqslant 0}$, given by

$$\begin{aligned}
\kappa_{\text{in},i}(y_i, \mu_i) &:= \left\lceil \max\left\{-\varsigma, \frac{\log\left(\max\{|y_i|, \Delta_{0,i}\}/(\ell_{\text{in},i}\mu_i)\right)}{\log \Omega_{\text{in},i}}\right\}\right\rceil \\
\kappa_{\text{out},i}(y_i, \mu_i) &:= \left\lceil \max\left\{-\varsigma, \frac{\log\left(|y_i|/(\ell_{\text{out},i}\mu_i)\right)}{\log \Omega_{\text{out},i}}\right\}\right\rceil
\end{aligned} \tag{31}$$

where

$$\ell_{\text{in},i} := \Omega_{\text{in},i}(M_i - \kappa_i\Delta_i), \qquad \ell_{\text{out},i} := M_i - \Delta_i \tag{32}$$

with κ_i as in (30), $\Delta_{0,i}$ as in (25), and where the constant $\varsigma \in (0, 1)$ can be chosen arbitrarily.

The functions $\kappa_{\text{in},i}$ and $\kappa_{\text{out},i}$ and the constants $\ell_{\text{in},i}$ and $\ell_{\text{out},i}$ are specified such that the following properties are satisfied. For all $y_i \in \mathbb{R}^{n_{y_i}}$ and $\mu_i \in \mathbb{R}_{\geqslant 0}$, $i \in \{1, 2, \ldots, l\}$, we have that:

a) $\kappa_{\text{in},i}(y_i, \mu_i), \kappa_{\text{out},i}(y_i, \mu_i) \subset \mathbb{N}$;
b) $\kappa_{\text{in},i}(y_i, \mu_i) \neq \{0\} \Rightarrow |y_i| < \ell_{\text{out},i}\mu_i$. Moreover, $\kappa_{\text{out},i}(y_i, \mu_i) = \{0\}$;
c) $\kappa_{\text{out},i}(y_i, \mu_i) \neq \{0\} \Rightarrow \ell_{\text{in},i}\mu_i < \max\{|y_i|, \Delta_{0,i}\}$. Moreover, $\kappa_{\text{in},i}(y_i, \mu_i) = \{0\}$.

Moreover, for each $\mu_i^+ \in \Omega_{\text{in},i}^{\kappa_{\text{in},i}(y_i,\mu_i)}\mu_i$ with $y_i \in \mathbb{R}^{n_{y_i}}$ and $\mu_i \in \mathbb{R}_{\geqslant 0}$, it holds that

d) $\frac{\Omega_{\text{in},i}}{\ell_{\text{in},i}} \max\{|y_i|, \Delta_{0,i}\} \leqslant \mu_i^+ \leqslant \frac{\max\{|y_i|, \Delta_{0,i}\}}{\ell_{\text{in},i}}$

and, for each $\mu_i^+ \in \Omega_{\text{out},i}^{\kappa_{\text{out},i}(y_i,\mu_i)}\mu_i$ with $y_i \in \mathbb{R}^{n_{y_i}}$ and $\mu_i \in \mathbb{R}_{\geqslant 0}$, it holds that

e) $\frac{|y_i|}{\ell_{\text{out},i}} \leqslant \mu_i^+ \leqslant \frac{\Omega_{\text{out},i}}{\ell_{\text{out},i}}|y_i|$.

Property (a) follows from the fact that $\lceil -\varsigma \rceil = \{0\}$ for any $\varsigma \in (0, 1)$. Properties (b) and (c) are due to the fact that according to (32) and (30), $0 < \ell_{\text{in},i} < \ell_{\text{out},i} < M_i$. At last, properties (d) and (e) follow directly from the definitions of $\kappa_{\text{in},i}(y_i, \mu_i)$ and $\kappa_{\text{out},i}(y_i, \mu_i)$, respectively. Let us remark that property (c) implies that $\kappa_{\text{in},i}(y_i, \mu_i) = 0$ when $\ell_{\text{in},i}\mu_i < \Delta_{0,i}$. As we will show, this property is important to ensure that the values of $\kappa_{\text{in},i}(y_i, \mu_i)$ and $\kappa_{\text{out},i}(y_i, \mu_i)$ remain finite all the time, especially when y_i crosses zero at any transmission instant t_k^i. Similar conditions have been used in [16], [33], and [36]. Moreover, observe that properties (b) and (c) imply that when the quantizer is updated, either a zoom-in or zoom-out event occurs or neither of them. It is worth mentioning, due to the fact that we only update the zoom variable μ_i at transmission instants, that the required number of zoom actions at each transmission instant, which will be transmitted over the network to the decoder, is directly affected by the length of the intertransmission times since the last transmission instant. In other words, it is expected that the longer the intertransmission time the more zoom actions need to be performed at the next transmission instant.

C. Stability Result

In this section, we present the main result. We are going to establish the following properties:

i) there exists a bounded set that is ISS, and in fact the tuning parameters $\Delta_{0,i}, \varepsilon_x, \nu_i, \vartheta_i$ in the algorithm, can be chosen to make this set arbitrarily small;
ii) the information transmitted over the network is bounded in each bounded time window, which implies the absence of Zeno behavior in transmission times and zoom in/out actions, i.e., the number of bits to be transmitted and the number of transmission instants are finite in each finite time window;
iii) the output measurement of each sensor remains within the range of its associated dynamic quantizer, i.e., quantizer saturation is avoided;
iv) the proposed approach prevents the redundant usage of the network due to quantization, in the sense that at each transmission instant it is guaranteed that the information to be transmitted from the sensor side is more accurate than what is available at the controller side.

In what follows, we will provide the corresponding formal results regarding these statements. We first define the following bounded set for which the ISS property will be ensured.

Definition 3: We define the following set $\mathcal{A} := \{\xi \in \mathbb{X} : R(\xi) \leqslant c\}$, where

$$R(\xi) := x^T Px + \sum_{i=1}^{l}\left(\gamma_i\tilde{\phi}_i(\tau_i)|e_i|^2 + \eta_i\right) \tag{33}$$

$$\tilde{\phi}_i(\tau_i) := \begin{cases} \phi_i(\tau_i) & \text{when } \tau \leqslant T_i \\ \phi_i(T_i) & \text{when } \tau > T_i \end{cases} \tag{34}$$

and $c := \frac{\sum_{i=1}^{l} \varepsilon_{y_i} \Delta_{0,i}^2}{\epsilon \min\{\varepsilon_x/\lambda_{\max}(P), 2\min_i \nu_i, \min_i \vartheta_i\}}$ with $P, \gamma_i, \varepsilon_x, \varepsilon_{y_i}$ as in Condition 1, $\Delta_{0,i}$ as in (12), and where $\epsilon \in (0,1)$ can be chosen arbitrarily. ■

We are ready to state the main result.

Theorem 1: Consider system (20) with the flow and the jump sets as in (19) with $\Psi_i, \eta_{0,i}$ specified in (25) and T_i defined in (27). Suppose that Assumption 1 and Condition 1 are satisfied and that the dynamic quantizer is designed as in (29)–(30). Let $\mathbb{X}_0 := \{\xi \in \mathbb{X} : \eta_i > 0, p_i = 0\}$. Then:

1) the set $\mathcal{A}$, as defined in Definition 3, is ISS w.r.t. w;
2) for each maximal solution pair (ξ, w) with $\xi(0,0) \in \mathbb{X}_0$ and $w \in \mathcal{L}_\infty$, it holds, when $p_i(t,j) = 1$, that $\kappa_{\text{in},i}(y_i(t,j), \mu_i(t,j)) \subseteq \{0, 1, \ldots, \kappa^*_{\text{in},i}\}$ and $\kappa_{\text{out},i}(y_i(t,j), \mu_i(t,j)) \subseteq \{0, 1, \ldots, \kappa^*_{\text{out},i}\}$, for some positive constants $\kappa^*_{\text{in},i}, \kappa^*_{\text{out},i}$. ■

Property 1 in Theorem 1 implies that an ISS property is guaranteed for the closed-loop system. In particular, in the absence of disturbances, the state trajectory converges to a neighbourhood of the origin whose size depends on $\sum_{i=1}^{l} \Delta_{0,i}$. This is due to the fact that μ_i does not eventually go to zero since no zooming in occurs when $\mu_i < \frac{\Delta_{0,i}}{\ell_{\text{in},i}}$ according to (12) in combination with (31), which is also the case in, e.g., [16], [33]. The set $\mathcal{A}$ in Definition 3, for which the ISS property is guaranteed, is bounded by the constant $c > 0$, which can be adjusted arbitrarily small by tuning the parameters $\Delta_{0,i}, \varepsilon_x, \nu_i, \vartheta_i$ of the event-triggering mechanism and of the dynamic quantizer appropriately. Property 2 in Theorem 1 shows that at transmissions, the elements of the sets $\kappa_{\text{in},i}(y_i, \mu_i)$ and $\kappa_{\text{out},i}(y_i, \mu_i)$, $i \in \{1, 2, \ldots, l\}$, are bounded by $\kappa^*_{\text{in},i}$ and $\kappa^*_{\text{out},i}$, respectively. The latter property is important to make sure that the amount of data sent over the network per transmission is bounded. Let us remark that the quantities $\bar{\mu}_i$ and $\bar{y}_i$, $i \in \{1, 2, \ldots, l\}$, represent upper bounds on $\|\mu_i\|_\infty$ and $\|y_i\|_\infty$, respectively. As shown in the proof of Theorem 1, the upper bounds $\kappa^*_{\text{in},i}$ and $\kappa^*_{\text{out},i}$ are given by

$$\kappa^*_{\text{in},i} := \max\left(\left\lceil \frac{\log\left(\Delta_{0,i}/(\ell_{\text{in},i}\bar{\mu}_i)\right)}{\log \Omega_{\text{in},i}} \right\rceil\right) \tag{35}$$

$$\kappa^*_{\text{out},i} := \max\left(\left\lceil \frac{\log\left(\bar{y}_i/(\ell_{\text{out},i}\underline{\mu}_i)\right)}{\log \Omega_{\text{out},i}} \right\rceil\right) \tag{36}$$

with

$$\bar{\mu}_i := \max\left\{\Omega_{\text{out},i}^{\kappa^*_{\text{out},i}} \frac{\bar{y}_i}{\ell_{\text{out},i}}, \mu_i(0,0)\right\} \tag{37}$$

$$\underline{\mu}_i := \frac{\Omega_{\text{in},i}\Delta_{0,i}}{\ell_{\text{in},i}} \tag{38}$$

and

$$\bar{y}_i := \sqrt{\frac{\lambda_{\max}(C_{p,i}^\top C_{p,i})}{\lambda_{\min}(P)}}\left(\sqrt{R(\xi(0,0))} + \sqrt{\frac{\varepsilon_w}{\rho}}\|w\|_\infty\right). \tag{39}$$

In addition to the result presented in Theorem 1, the proposed conditions also lead to the following favorable properties which have a key role in the proof of Theorem 1.

Corollary 1: Consider system (20) with the flow and the jump sets as in (19) with $\Psi_i, \eta_{0,i}$ specified in (25) and T_i defined in (27). Suppose that Assumption 1 and Condition 1 are satisfied and that the dynamic quantizer is designed as in (29)–(30). Let $\mathbb{X}_0 := \{\xi \in \mathbb{X} : \eta_i > 0, p_i = 0\}$. Then, for each maximal solution pair (ξ, w) with $\xi(0,0) \in \mathbb{X}_0$ and $w \in \mathcal{L}_\infty$, it holds that, when $p_i(t,j) = 1$:

3) $|y_i(t,j)| \leqslant M_i \mu_i(t,j)$;
4) $|e_{s,i}(t,j)| > |e_{q,i}(t,j)|$. ■

Property 3 in Corollary 1 implies that at each transmission event, the output measurement y_i is within the range of the associated quantizer. As a consequence, the quantization error is always smaller than or equal to the quantization error bound at each transmission event. Property 4 in Corollary 1 implies that at each transmission event, i.e., when $\xi \in \mathcal{D}_i$ and $p_i = 1$, $i \in \{1, 2, \ldots, l\}$, the magnitude of the sampling-induced error is larger than the error due to quantization, which implies that the transmitted information is more accurate than the information already available at the corresponding receiving node. As such, property 4 helps in avoiding redundant usage of the network.

Remark 3: We note from (38) that the constant parameter $\Delta_{0,i} > 0$ acts to provide a lower bound $\underline{\mu}_i$ on the zoom variable $\mu_i, i \in \{1, 2, \ldots, l\}$. This lower bound $\underline{\mu}_i$ is still needed even though the zoom variable μ_i is only updated at transmission instants, which automatically rules out Zeno behavior on the zoom actions thanks to the enforced minimum time T_i between two transmissions. The lower bound $\underline{\mu}_i$ is rather introduced to limit the size of the transmitted data packages, which is the purpose of quantization. Otherwise, if the state is in equilibrium and μ_i is infinitesimal, small disturbances on the plant may require an infinite number of zoom-out actions, which implies that the data package that has to be transmitted is of infinite size.

Remark 4: It is important to emphasize that the problem stated in Section III-D cannot be solved in a straightforward manner by a direct combination of existing techniques on event-triggered control, e.g., [25] and on dynamic quantization, e.g., [16], [39], for different reasons. First, the interaction between the event-triggered implementation and the dynamic quantization produces new phenomena, which can have negative impact on the stability analysis and/or the efficient utilization of the network. For instance, due to the quantization effect, the sampling-induced error e_i at each channel $i \in \{1, 2, \ldots, l\}$ is not necessarily reset to zero at each transmission instant $t_k^i, k \in \mathbb{N}$, see (14), which often forms an important argument in the stability analysis of event-triggered control systems, see, e.g., [17], [25], [44]. Hence, this issue is not trivial to handle and requires careful construction of both the design strategy, see (12), (25), (28), (29), and the Lyapunov function candidate in order to guarantee closed-loop stability, see (52) in the proof of Theorem 1 in the Appendix. Second, since the zoom-out actions are output dependent and since the plant is subject to external disturbances, it is challenging to ensure that the quantization variable remains bounded, which is necessary to achieve an ISS property, see, e.g., [16], [39]. The technique of [16] is developed for the continuous-time case and relies on the fact the full state vector can be measured while the implementation setup in [39]

is different from the one we consider in this study and hence, they cannot be directly applied to our case. Moreover, since the zoom-in actions are also output dependent, the quantization strategy must be carefully designed in order to avoid Zeno behavior on the quantization events, in particular when the output trajectory crosses zero, as confirmed later on simulation. Given these and other reasons, the joint design of the event-triggered controller and the dynamic quantizer is intricate and its easy to make design choices in which important properties such as ISS or non-Zenoness are lost, which hamper practical applicability.

D. Design Procedure of the Event-Triggering Mechanism (ETM) and Quantizer

In this section, we discuss the design of the ETM and the dynamic quantizer. In view of (27) and (29), the design parameters $\tilde{\gamma}_i, \varepsilon_{y_i}, \lambda_i, \tilde{\lambda}_i$ $i \in \{1, 2, \ldots, l\}$ create a strong coupling between the design of the event-triggering mechanism and the design of the dynamic quantizer.

The first step of the design procedure is to find suitable γ_i, $i \in \{1, 2, \ldots, l\}$, by minimizing the weighted sum $\sum_{i=1}^{l} \pi_i \gamma_i$ subject to (23) with $\pi_i \in (0, 1)$, $i \in \{1, 2, \ldots, l\}$, such that $\sum_{i=1}^{l} \pi_i = 1$. The selection of π_i allows to balance the communication resource utilization among the different nodes. The parameters $\Omega_{\text{in},i}$ and $\Omega_{\text{out},i}$, $i \in \{1, 2, \ldots, l\}$ allow to balance the required number of quantization regions that is needed to satisfy (30) and the maximum number of zoom-in and zoom-out events per transmission as given in (35) and (36), respectively. The next step is to select κ_i as small as possible to minimize the lower bound on M_i/Δ_i as given in (30). The latter is desired as M_i/Δ_i typically reflects the number of quantization regions. After $\Omega_{\text{in},i}$, $\Omega_{\text{out},i}$, and κ_i, $i \in \{1, 2, \ldots, l\}$ are obtained, we take M_i, Δ_i such that (30) holds. Finally, the tuning of λ_i can be used to obtain an intuitive tradeoff between the number of transmissions and the amount of data that needs to be transmitted per transmission. When λ_i is reduced, the value of T_i in (27) will increase and, depending on the choice of $\tilde{\lambda}_i$, the value of $\tilde{\gamma}$ will decrease, which may result in a reduction in the amount of transmissions. However, by reducing λ_i, the right-hand side of (29) will also increase. Hence, the value of $\frac{M_i}{\Delta_i}$ needs to be increased which typically implies that more quantization regions are required, in order to ensure that (29) holds. We will illustrate this also with an example in the next section. The design procedure is summarized in the following algorithm.

Algorithm 1: Design Procedure.

For each node $i \in \{1, 2, \ldots, l\}$

1: pick $\pi_i \in (0, 1)$ such that $\sum_{i=1}^{l} \pi_i = 1$
2: minimize $\sum_{i=1}^{l} \pi_i \gamma_i$ subject to (23) and compute the parameters $\varepsilon_{y_i}, \gamma_i$
3: pick $\nu_i, \vartheta_i, \Delta_{0,i} > 0$ in (25) sufficiently small and take $\lambda_i \in (0, 1)$, $\tilde{\lambda}_i \in [\lambda_i, \lambda_i^{-1})$ in (27) to achieve the desired tradeoff between performance and bit length, see (33), (35), (36) and Remark 2
4: compute the time T_i and the parameters of (25) for the event-triggering mechanism (8)–(9)
5: take $\kappa_i > 1$ sufficiently small and $\Omega_{\text{in},i} \in (0, 1)$ in (29)
6: choose $M_i, \Delta_i > 0$, such that (29) is satisfied
7: take $\Omega_{\text{out},i} > 1$ such that (30) holds

VI. Illustrative Example

We consider the following linearized model of an inverted pendulum with a cart system, taken from [45], affected by external disturbances

$$\dot{x}_p = \begin{bmatrix} 0 & 1 & 0 & 0 \\ 0 & -0.1789 & 7.7447 & 0 \\ 0 & 0 & 0 & 1 \\ 0 & -0.5263 & 51.5789 & 0 \end{bmatrix} x_p + \begin{bmatrix} 0 \\ 1.7895 \\ 0 \\ 5.2632 \end{bmatrix} u + \begin{bmatrix} 1 \\ 0 \\ 1 \\ 0 \end{bmatrix} w$$
$$y = \begin{bmatrix} 1 & 0 & 0 & 0 \\ 0 & 0 & 1 & 0 \end{bmatrix} x_p \tag{40}$$

where x_{p_1} is the cart position, x_{p_2} is the cart velocity, x_{p_3} is the pendulum angle from vertical, x_{p_4} is the pendulum angular velocity, u is the input force, and w is the external disturbance. The numerical values in the matrices A_p, B_p, C_p correspond to a mass cart of $M = 0.5$ kg, pendulum mass $m = 0.5$ kg, pendulum length $l = 0.3$ m, pendulum inertia $I = 0.006$ kgm^2, and cart surface friction $b = 0.1$ N/m/s. Interestingly, the open-loop system is unstable, and the disturbances affect the states that are not directly affected by the input.

In [45], the plant is stabilized by an observer-based controller of the form

$$\dot{\hat{x}} = A_p \hat{x} + B_p u + L(y - C_p \hat{x}), \quad u = K\hat{x} \tag{41}$$

where $\hat{x} \in \mathbb{R}^4$ is the observer state, $L \in \mathbb{R}^{4\times 2}$ is the observer gain, and $K \in \mathbb{R}^{1\times 4}$ is the controller gain. The values of L, K in [45] are given by

$$L = \begin{bmatrix} 11.0993 & -0.0991 \\ 29.7908 & 2.1306 \\ -0.5518 & 11.3189 \\ -5.5941 & 63.2481 \end{bmatrix},$$

$K = [17.0386 \;\; 13.0877 \;\; -50.0520 \;\; 9.8150]$.

By considering that the plant output y is quantized and transmitted asynchronously over two different channels and by following similar steps as in Section IV, we obtain model (15), (17) with (note from (7), (41) that $D_c = 0$ in this case) $\mathcal{A}_1 = \left[\begin{smallmatrix} A_p & B_pK \\ LC_p & A_p + B_pK - LC_p \end{smallmatrix}\right]$, $\mathcal{B}_1 = \left[\begin{smallmatrix} 0 \\ L \end{smallmatrix}\right]$, $\mathcal{E}_1 = \left[\begin{smallmatrix} E_p \\ 0 \end{smallmatrix}\right]$, $\mathcal{A}_2 = [-C_pA_p - C_pB_pK]$, $\mathcal{B}_2 = [0]$, and $\mathcal{E}_2 = [-C_pE_p]$. The matrix $\mathcal{A}_1$ is Hurwitz by design and hence, we know that the LMI (23) is feasible for some symmetric real matrix P, real numbers $\varepsilon_x, \varepsilon_w > 0$ and $\varepsilon_{y_i}, \gamma_i > 0$ for $i \in \{1, 2\}$. Following Algorithm 1 and by solving the LMI (23), we obtain $\varepsilon_{y_1} = 4.4414$, $\varepsilon_{y_2} = 39.7353$, $L_1 = L_2 = 0$, $\gamma_1 = 70.4173$, and $\gamma_2 = 119.0389$. We take $\lambda_1 = \lambda_2 = 0.5$, $\tilde{\lambda}_1 = 0.6, \tilde{\lambda}_2 = 0.8$, $\nu_1 = \nu_2 = 0.01$ and we compute the values of T_1, T_2 by using (27), which yields $T_1 = 0.0076$ and $T_2 = 0.0035$. Furthermore, we obtain $\tilde{\gamma}_1 = 6744$ and $\tilde{\gamma}_2 = 2324$. Finally, we set $\vartheta_1 = \vartheta_2 = 0.01$ and hence, all the required parameters for the event-triggering functions

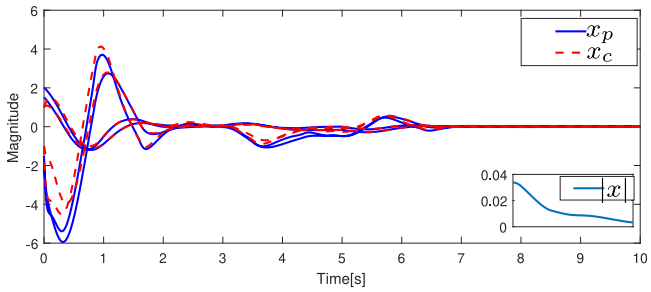

Fig. 2. State trajectory for the plant and the controller.

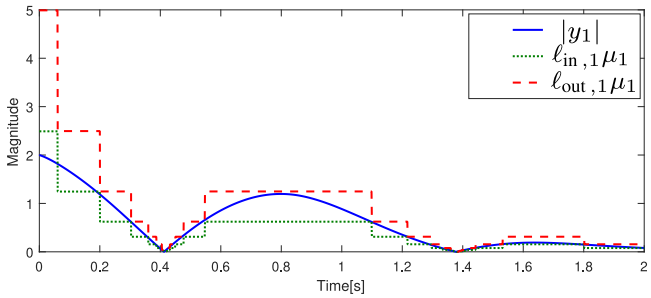

Fig. 3. Zoom actions for y_1 for the first two seconds.

in (25) are defined. Next, we set the range of the quantizers to be $M_1 = 50, M_2 = 50$ and we take $\Delta_1 = 0.1$, $\Delta_2 = 0.2$, $\Delta_{01} = \Delta_{02} = 1 \times 10^{-6}$, $\Omega_{\text{in},1} = \Omega_{\text{in},2} = 0.5, \Omega_{\text{out},1} = \Omega_{\text{out},2} = 2$, and $\kappa_1 = \kappa_2 = 2$, which verify conditions (29), (30) and lead to $\ell_{\text{in},1} = 24.9$, $\ell_{\text{in},2} = 24.8$, $\ell_{\text{out},1} = 49.9$, and $\ell_{\text{out},2} = 49.8$. We run simulations for 10 s with the initial conditions $x(0,0) = (2, -2, 1.5, -1.5, 1, -1, 1, -1)$, $e(0,0) = (0,0)$, $\eta(0,0) = (0,0)$, $\phi(0,0) = (\lambda_1^{-1}, \lambda_2^{-1})$, $\mu(0,0) = (1,1)$ and with the external disturbance w satisfying $w(t,j) = 2\sin(2\pi t)$ for all $(t,j) \in \operatorname{dom} w$ with $t \in [0,1]$, $w(t,j) = 0$ for all $(t,j) \in \operatorname{dom} w$ with $t \in (1,3]$ and $w(t,j) = 0.2$ for all $(t,j) \in \operatorname{dom} w$ with $t \in (3,5]$. The observed minimum and average intertransmission times, respectively, denoted by $\tau_{\min}$ and τ_{avg}, for node 1 are $\tau_{\min,1} = 0.0089$, $\tau_{\text{avg},1} = 0.0266$ and for node 2 are $\tau_{\min,2} = 0.0036$, $\tau_{\text{avg},2} = 0.0161$.

We note that $\tau_{\min,1} > T_1$ while $\tau_{\min,2} \approx T_2$, which supports the observation of Remark 2 on the choice of $\tilde{\lambda}_i$ since $\tilde{\lambda}_1 > \lambda_1$ and $\tilde{\lambda}_2 = \lambda_2$. The state trajectories of the plant and the dynamic controller are shown in Fig. 2, where we note that the state converges to a small neighborhood of the origin as expected. The zoom-in/zoom-out events by the respective dynamic quantizers are shown in Figs. 3 and 4 during the first seven seconds. We note that at any transmission instant $t_k^i, k \in \mathbb{N}$, only a zoom-in event or a zoom-out event occurs but not both of them due to the design conditions in Section V-B that imply properties (b) and (c) below (38). Figs. 5 and 6 present the generated transmission instants and the zoom instants during the first three seconds for nodes 1 and 2, respectively. We observe that the zoom actions are only executed at transmission instants as described in Section III-C and that at some transmission instants, no zoom action occurs. The latter is the case when none of the zoom conditions are met at those instants. The tradeoff between transmissions and number of quantization regions is illustrated in Figs. 7 and 8 for node 1 and 2, respectively. These figures are generated by varying λ_i in (27), (29) from 0.01 to 0.99 and by taking $\tilde{\lambda}_i = \lambda_i$. Observe that larger values of $\frac{M_i}{\Delta_i}, i \in \{1,2\}$, which for this case imply more quantization regions, lead to larger values of the guaranteed minimum time T_i between two consecutive transmissions/zooms at the corresponding node and vice versa, as discussed in Section V-D.

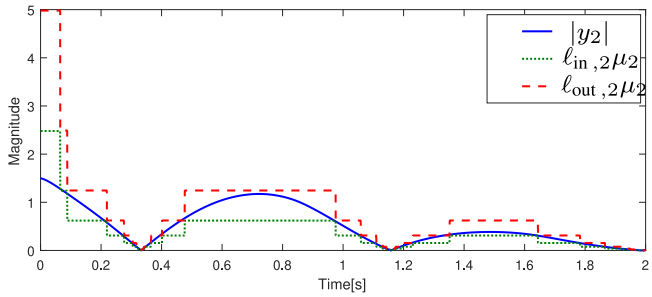

Fig. 4. Zoom actions for y_2 for the first three seconds.

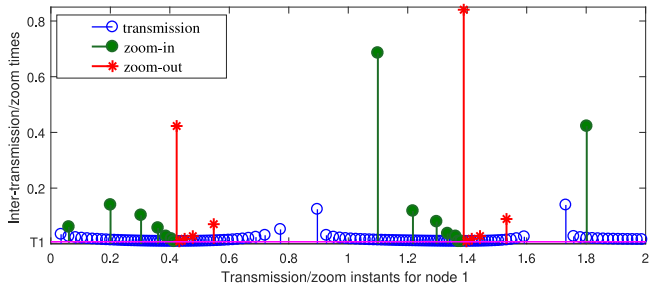

Fig. 5. Transmission/zoom instants for y_1 for the first two seconds.

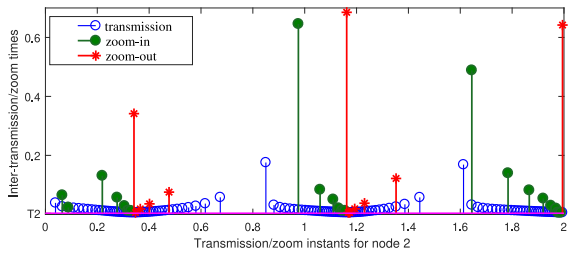

Fig. 6. Transmission/zoom instants for y_2 for the first two seconds.

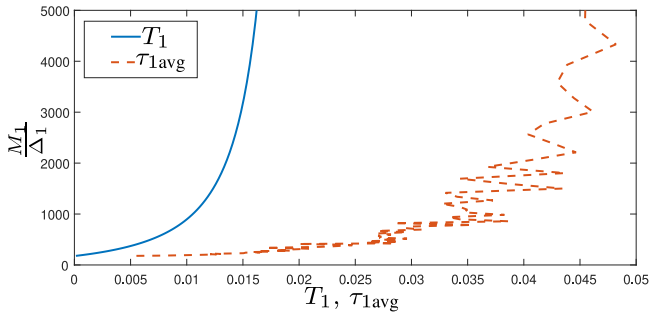

Fig. 7. Tradeoff curves between number of quantization regions and transmissions for y_1.

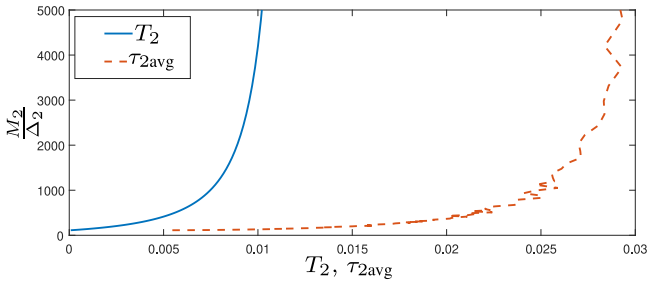

Fig. 8. Tradeoff curves between number of quantization regions and transmissions for y_2.

VII. Conclusion

In this paper we addressed the problem of input-to-state stabilization of linear systems over digital communication networks. We considered three important features of the communication network. First of all, our problem involved quantization of the measured variables to have a finite number of bits to be transmitted in packets. Second, we employed a resource-aware control paradigm (in particular, event-triggered control) to utilise the bandwidth-limited communication channels only when needed. Third, we studied the scenario where multiple sensor nodes transmit their information asynchronously. We provided a complete design solution for this setup for a linear plant in the presence of disturbances and only based on output measurements. Our main design framework solves the codesign problem of synthesising both the dynamic quantizers and the transmission policies via the event-triggering mechanisms that are provided for each individual sensor node. The resulting closed-loop system has the ISS property with an ISS set of which the size can be made arbitrarily small by appropriate selection of the tuning parameters of the event-triggering/dynamic quantization combination (hence, we have "global practical ISS"). The design approach applies to any stabilizable and detectable linear plant (and any corresponding stabilizing controller) and is systematic in nature. Interestingly, the intuitive tradeoff between the number of quantization levels (and thus the size of the information/data packet that has to be transmitted) and the number of transmissions naturally appears in our main theoretical results and the design methods. In fact, the design of the dynamic quantizers and the event generators is directly coupled and reflects this essential tradeoff. The proposed event-triggering mechanism enforces the existence of a strictly positive lower bound on the intertransmission times of each channel, which prevents the occurrence of Zeno behavior. Moreover, the dynamic quantization strategy prevents the accumulation of zoom actions since the zoom actions only take place at transmission instants. The zoom parameter of the dynamic quantizer is shown to be always bounded. The chattering between the zoom-in stage and the zoom-out stage is avoided and the redundant access of the network is prevented.

The framework laid down in this paper can be extended in different directions, such as the inclusion of delays based on the work in [2], combined with codesign of the controllers [46]. Also, it might be the case in some practical scenarios that the event-triggering mechanism only has access to the quantized output measurement but not the current (true) value of the plant output as we have considered in this study. This would call for a new analysis corresponding to the case where in Fig. 1 the sensor and the encoder are reversed in the control loop. Also the extension of the approach to nonlinear systems is a challenging and a relevant problem for the future, although the Lyapunov-based approach put forward here, gives good hints to solve this problem as well.

Appendix

In order to streamline the proof of Theorem 1, we first present the proof of Corollary 1. In the proofs, we often omit the time arguments of the solution ξ of hybrid system $\mathcal{H}$ and we do not mention $\operatorname{dom}\xi$ explicitly.

Proof of Corollary 1. Proof of Statement 3: By recalling that $\mathbb{X}_0 := \{\xi \in \mathbb{X} : \eta_i > 0, p_i = 0\}$, we can see from (21) that $p_i(t,j) = 1$ is only possible if the system has jumped according to the jump map $G_i^\mu(\xi)$. To be more concrete, we can conclude from (21) that for all $(t,j) \in \operatorname{dom}\xi$ for which $p_i(t,j) = 1$, there exists an $n \in \mathbb{N}$ such that $\xi(t, j-n) \in G_i^\mu(\mathcal{D}_i)$ and that $\xi(t,\bar{j}) \in \bigcup_{k\in\{1,2,\ldots,l\}\setminus\{i\}} (\{G_k^\mu(\mathcal{D}_i)\} \cup \{G_k^y(\mathcal{D}_i)\})$ for all $\bar{j} \in \{j-n+1,\ldots,j\}$. Since μ_i is only affected by the jump map $G_i^\mu(\mathcal{D}_i)$ (corresponding to a zoom-update event at node i), we only need to show that $|y_i(t,j)| \leqslant M_i\mu_i(t,j)$ for all $\xi(t,j) \in G_i^\mu(\mathcal{D}_i)$ with $(t,j) \in \operatorname{dom}\xi$. To do so, we consider the cases that a zoom-in event occurs, a zoom-out event occurs, and that none of the zoom conditions are violated.

In case of a zoom-in event, i.e., when $\xi \in \mathcal{D}_i$, and the system jumps according to $\xi \in G_i^\mu(\xi)$ with $\mu_i^+ \in \Omega_{\text{in},i}^{\kappa_{\text{in},i}(y_i,\mu_i)}\mu_i$ and $y_i^+ = y_i$, we have that

$$\ell_{\text{out},i}\mu_i^+ \overset{(31)}{\geqslant} \Omega_{\text{in},i}\tfrac{\ell_{\text{out},i}}{\ell_{\text{in},i}}\max\{|y_i|,\Delta_{0,i}\} \overset{(32)}{\geqslant} \tfrac{M_i-\Delta_i}{M_i-\kappa_i\Delta_i}|y_i|. \tag{42}$$

Since according to (30), $\kappa_i > 1$, we obtain that $\ell_{\text{out},i}\mu_i^+ \overset{(42)}{\geqslant} |y_i|$ and thus, $M_i\mu_i^+ \geqslant |y_i^+|$.

In case of a zoom-out event, i.e., when $\xi(t,j) \in \mathcal{D}_i$ and the system jumps according to $\xi^+ \in G_i^\mu(\xi)$ with $\mu_i^+ \in \Omega_{\text{out},i}^{\kappa_{\text{out},i}(y_i,\mu_i)}\mu_i$ and $y_i^+ = y_i$, it immediately follows from (31) that $\ell_{\text{out},i}\mu_i^+ \geqslant |y_i^+|$ and thus, $M_i\mu_i^+ \geqslant |y_i^+|$ as $\ell_{\text{out},i} = M_i - \Delta_i \leqslant M_i$.

In case none of the zoom conditions are violated, i.e., when $\xi \in \mathcal{D}_i$ and the system jumps according to $\xi^+ \in G_i^\mu(\xi)$ with $\mu_i^+ = \mu_i$ and $y_i^+ = y_i$ we have that $\kappa_{\text{out},i}(y_i,\mu_i) = 0$ which, per definition of $\kappa_{\text{out},i}$, implies that $|y_i| \leqslant \ell_{\text{out},i}\mu_i$ and thus $M_i\mu_i^+ \geqslant |y_i^+|$. Hence, statement 3 in Corollary 1 holds.

Proof of Statement 4: Consider the following claim.

Claim 1: Let the hypotheses of Theorem 1 hold. Consider a solution pair (ξ, w) to (20) with $\xi(0,0) \in \mathbb{X}_0$ with $\mathbb{X}_0$ as defined in Theorem 1. Then, it holds for all $(t,j) \in \operatorname{dom}\xi$ with $\xi(t,j) \in \mathcal{D}_i$ that $\tilde{\gamma}_i|e_i(t,j)|^2 \geqslant \varepsilon_{y_i}\max\{|y_i^2(t,j)|, \Delta_{0,i}^2\}$, $i \in \{1,2,\ldots,l\}$. ■

Proof of Claim 1: To prove this claim, we use the following lemma.

Lemma 1: Consider $f : \mathbb{R}_{\geq 0} \to \mathbb{R}$ that is continuously differentiable at an open interval containing $(T_1, T_2]$ with $f(t) \geqslant 0$ $t \in (T_1, T_2]$ for $T_2 > T_1 > 0$ and $f(T_2) = 0$, then $\dot{f}(T_2) \leqslant 0$. ■

Moreover, let us define $\bar{E}_i := \{(t,j) \in \operatorname{dom}\xi : \xi(t,j) \in \mathcal{C} \cap \mathcal{D}_i\}$ for all $i \in \{1,2,\dots,l\}$. Observe from (25) that $\Psi_i(o_i(t,j)) > 0$ for all $(t,j) \in \operatorname{dom}\xi$ for which $\eta_i(t,j) = 0$ and $0 \leqslant \tau_i(t,j) < T_i$. By means of the latter, and by recalling (9) and the fact that, as per definition of $\mathbb{X}_0$, $\eta_i(0,0) > 0$ for all $i \in \{1,2,\dots,l\}$, we obtain that $\eta_i(t,j) > 0$ for all $(t,j) \in \operatorname{dom}\xi$ for which $\tau_i(t,j) = T_i$. Since $\eta_i(t,j) = 0$ and $\tau_i(t,j) \geqslant T_i$ when $\xi(t,j) \in \mathcal{D}_i$, we can consequently conclude that for each $(t,j) \in \bar{E}_i$, there exists a $t' < t$ such that $(t',j) \in \mathcal{C}$ with $\tau_i(t',j) > T_i$. By using the latter, the fact that, for all $(t,j) \in \operatorname{dom}\xi$, $\eta_i(t,j) \geqslant 0$, as per definition of $\mathbb{X}$ and Lemma 1, we obtain that for all $(t,j) \in \bar{E}_i$, $\dot{\eta}(t,j) \leqslant 0$. Observe from (25) that $\dot{\eta}_i(t,j) \geqslant \varepsilon_{y_i} \max\left\{|y_i(t,j)|^2, \Delta_{0,i}^2\right\} - \tilde{\gamma}_i |e_i(t,j)|^2 - \vartheta_i \eta_i(t,j)$ for all $(t,j) \in \operatorname{dom}\xi$. Hence, we have that for all $i \in \{1,2,\dots,l\}$, and all $(t,j) \in \bar{E}_i$, $\tilde{\gamma}_i |e_i(t,j)|^2 \geqslant \varepsilon_{y_i} \max\{|y_i^2(t,j)|, \Delta_{0,i}^2\}$.

To complete the proof, we need to show that the property $\tilde{\gamma}_i |e_i(t,j)|^2 \geqslant \varepsilon_{y_i} \max\{|y_i^2(t,j)|, \Delta_{0,i}^2\}$ also holds for all $(t,j) \in \operatorname{dom}\xi$ for which $\xi(t,j) \in \mathcal{D}_i \setminus \mathcal{C}$. Observe that $\xi(t,j) \in \mathcal{D}_i \setminus \mathcal{C}$ implies that $p_i(t,j) = 1$ for all $(t,j) \in \operatorname{dom}\xi$. As mentioned earlier, $p_i(t,j) = 1$ implies that there exists an $n \in \mathbb{N}$ such that $\xi(t, j-n) = G_i^{\mu}(\mathcal{D}_i)$ and that $\xi(t,\bar{j}) \in \bigcup_{k \in \{1,2,\dots,l\} \setminus \{i\}} (\{G_k^{\mu}(\mathcal{D}_i)\} \cup \{G_k^{y}(\mathcal{D}_i)\})$ for all $\bar{j} \in \{j-n+1, \dots, j\}$. Since y_i and e_i are not affected after the jump maps $G_i^{\mu}(\xi)$ or $G_k^{y}(\xi)$, $i \in \{1,2,\dots,l\}$, $k \in \{1,2,\dots,l\} \setminus \{i\}$ are applied, Claim 1 follows. ■

Claim 2: Let the hypotheses of Theorem 1 hold. Consider a solution pair (ξ, w) to (20) with $\xi(0,0) \in \mathbb{X}_0$ with $\mathbb{X}_0$ as defined in Theorem 1. Then, it holds for all $(t,j) \in \operatorname{dom}\xi$ with $p_i(t,j) = 1$ that $\ell_{\text{in},i} \mu_i(t,j) \leqslant \max\{|y_i(t,j)|, \Delta_{0,i}\}$. ■

Proof of Claim 2: Following similar arguments as in the proof of statement 2, we only need to show that $\ell_{\text{in},i} \mu_i \leqslant \max\{|y_i|, \Delta_{0,i}\}$ for all $\xi \in G_i^{\mu}(\mathcal{D}_i)$. To do so, we consider three cases, namely, the cases that a zoom-in event occurs, that a zoom-out event occurs, and that none of the zoom conditions are violated.

In case of a zoom-in event, i.e., when $\xi \in \mathcal{D}_i$ and the system jumps according to $\xi^+ \in G_i^{\mu}(\xi)$ with $\mu_i^+ \in \Omega_{\text{in},i}^{\kappa_{\text{in},i}(y_i,\mu_i)} \mu_i$ and $y_i^+ = y_i$, we can immediately conclude from (31) that $\ell_{\text{in},i} \mu_i^+ \leqslant \max\{|y_i^+|, \Delta_{0,i}\}$.

In case of a zoom-out event, i.e., when $\xi \in \mathcal{D}_i$ and the system jumps according to $\xi^+ \in G_i^{\mu}(\xi)$ with $\mu_i^+ \in \Omega_{\text{out},i}^{\kappa_{\text{out},i}(y_i,\mu_i)} \mu_i$ and $y_i^+ = y_i$, we obtain that

$$\ell_{\text{in},i} \mu_i^+ \overset{(31)}{\leqslant} \Omega_{\text{out},i} \tfrac{\ell_{\text{in},i}}{\ell_{\text{out},i}} |y_i| \overset{(32)}{=} \Omega_{\text{out},i} \Omega_{\text{in},i} \tfrac{M_i - \kappa_i \Delta_i}{M_i - \Delta_i} |y_i| \overset{(30)}{\leqslant} \max\{|y_i^+|, \Delta_{0,i}\}. \tag{43}$$

Let us remark that for the last inequality, we used the fact that the bound on κ_i given in (30) is such that $\Omega_{\text{out},i} \Omega_{\text{in},i} \frac{M_i - \kappa_i \Delta_i}{M_i - \Delta_i} < 1$.

Finally, we consider the case that no zoom condition is violated, i.e., when $\xi \in \mathcal{D}_i$ and the system jumps according to $\xi^+ \in G_i^{\mu}(\xi)$ with $\mu_i^+ = \mu_i$ and $y_i^+ = y_i$. In this case $\kappa_{\text{in},i}(y_i,\mu_i) = \kappa_{\text{out},i}(y_i,\mu_i) = \{0\}$, and thus, it holds trivially that $\ell_{\text{in},i} \mu_i^+ \leqslant \max\{|y_i^+|, \Delta_{0,i}\}$, which completes the proof of Claim 2. ■

To complete the proof of statement 3, we proceed with observing that in view of (29), $M_i - \kappa_i \Delta_i \geqslant \frac{2\sqrt{\tilde{\gamma}_i}}{\sqrt{\varepsilon_{y_i}} \Omega_{\text{in},i} \lambda_i} \Delta_i$. Hence, in view of the definition of $\ell_{\text{in},i}$ in (32), we have $2\Delta_i \frac{\sqrt{\tilde{\gamma}_i}}{\lambda_i \sqrt{\varepsilon_{y_i}}} \leqslant \Omega_{\text{in},i}(M_i - \kappa_i \Delta_i) = \ell_{\text{in},i}$. Hence, $\frac{2\Delta_i}{\lambda_i} \leqslant \frac{\sqrt{\varepsilon_{y_i}} \ell_{\text{in},i}}{\sqrt{\tilde{\gamma}_i}}$. By multiplying both sides by $\mu_i(t,j)$ we have that, for all $\xi(t,j) \in \mathcal{D}$ for which $p_i(t,j) = 1$ with $(t,j) \in \operatorname{dom}\xi$, $\frac{2\Delta_i \mu_i(t,j)}{\lambda_i} \leqslant \frac{\sqrt{\varepsilon_{y_i}} \ell_{\text{in},i} \mu_i(t,j)}{\sqrt{\tilde{\gamma}_i}}$, which leads to

$$\tfrac{2\Delta_i \mu_i(t,j)}{\lambda_i} \overset{\text{Claim 2}}{\leqslant} \tfrac{\sqrt{\varepsilon_{y_i}} \max\{|y_i(t,j)|, \Delta_{0,i}}}{\sqrt{\tilde{\gamma}_i}} \overset{\text{Claim 1}}{\leqslant} |e_i(t,j)| \overset{(13)}{\leqslant} |e_{s,i}(t,j)| + |e_{q,i}(t,j)|. \tag{44}$$

By means of statement 2 of Theorem 1 and (10), we obtain that $|e_{q,i}(t,j)| \leqslant \Delta_i \mu_i(t,j)$ for all $\xi(t,j) \in \mathcal{D}$ for which $p_i(t,j) = 1$ with $(t,j) \in \operatorname{dom}\xi$. Combining the latter fact with (44) yields $|e_{s,i}(t,j)| \geqslant \frac{2-\lambda_i}{\lambda_i} \Delta_i \mu_i(t,j)$ for all $\xi(t,j) \in \mathcal{D}$ for which $p_i(t,j) = 1$ with $(t,j) \in \operatorname{dom}\xi$. Since $\lambda_i \in (0,1)$, it holds that, for all $\xi(t,j) \in \mathcal{D}_i \wedge p_i(t,j) = 1$, $|e_{s,i}(t,j)| > \Delta_i \mu_i(t,j) \geqslant |e_{q,i}(t,j)|$. Thus, statement 4 of Corollary 1 is proven.

All the statements of Corollary 1 are now proved. ■

Proof of Theorem 1. Proof of Statement 1: To prove the ISS property of the set $\mathcal{A}$, we show that there exists an ISS Lyapunov function U for the hybrid system $\mathcal{H}$ described by (19) and (20). To be more specific, we aim to find a locally Lipschitz nonnegative function U that satisfies the following properties. For some functions $\alpha_1, \alpha_2 \in \mathcal{K}_\infty$ such that for all $\chi \in \mathcal{C} \cup \mathcal{D} \cup G(\mathcal{D})$, it holds that

$$\alpha_1(|\chi|_{\mathcal{A}}) \leqslant U(\chi) \leqslant \alpha_2(|\chi|_{\mathcal{A}}). \tag{45}$$

Moreover, for each solution pair (ξ, w) with $\xi(0,0) \in \mathbb{X}_0$ and $w \in \mathcal{L}_\infty$, there exist some functions $\tilde{\rho} \in \mathcal{K}_\infty$ and $\sigma \in \mathcal{K}$, such that for all $(t,j) \in \operatorname{dom}\xi$, it holds that when $\xi(t,j) \in \mathcal{D}$

$$U(G(\xi(t,j))) - U(\xi(t,j)) \leqslant 0 \tag{46}$$

and for almost all $(t,j) \in \operatorname{dom}\xi$, when $\xi(t,j) \in \mathcal{C}$, it holds that

$$\langle \nabla U \xi(t,j), F(\xi(t,j), w(t,j)) \rangle \leqslant -\tilde{\rho}(U(\xi(t,j))) + \sigma(|w(t,j)|). \tag{47}$$

Observe that the above-mentioned ISS conditions are closely related to the ISS conditions presented in [47, Def. 3.2]. The ISS condition in (45)–(47) are relaxed compared to [47]. This is possible as we will have that all the maximal solutions of $\mathcal{H}$ described by (19) and (20) are t-complete, see also [29, Prop. 3.27], [7, Lemma III.3], [48].

Consider the function $U(\xi) := \max\{0, R(\xi) - c\}$ with the function R as in Theorem 1. Observe that $U(\xi) = 0$ for $\xi \in \mathcal{A}$. Moreover, in view of (28) and (34), $\tilde{\phi}_i(\tau_i(t,j)) > 0$ for all $(t,j) \in \operatorname{dom}\xi$ and $i \in \{1,2,\dots,l\}$. Hence, since $\eta_i(t,j) \geqslant 0$ for all $(t,j) \in \operatorname{dom}\xi$ in view of the definition of $\mathbb{X}$, we deduce that the function U satisfies the inequality in (45) and thereby, constitutes an appropriate candidate ISS Lyapunov function.

Lemma 2: For all $\xi \in \mathcal{C} \setminus \mathcal{A}$, it holds that

$$\epsilon \left(\varepsilon_x |x|^2 + \sum_{i=1}^{l} 2\nu_i \gamma_i \tilde{\phi}_i(\tau_i)|e_i|^2 + \sum_{i=1}^{l} \vartheta_i \eta_i \right) \geqslant \sum_{i=1}^{l} \varepsilon_{y_i} \Delta_{0,i}^2. \tag{48}$$

Proof of Lemma 2: In view of the definition of $\mathcal{A}$, it holds for all $\xi \in \mathcal{C} \setminus \mathcal{A}$ that $R(\xi) \geqslant c$ with c as defined in Theorem 1, i.e.,

$$x^\top P x + \sum_{i=1}^{l} \left(\gamma_i \tilde{\phi}_i(\tau_i)|e_i|^2 + \eta_i \right) \geqslant \frac{\sum_{i=1}^{l} \varepsilon_{y_i} \Delta_{0,i}^2}{\epsilon \min\{\varepsilon_x/\lambda_{\max}(P),\, 2\min_i\, \nu_i,\, \min_i\, \vartheta_i\}}. \tag{49}$$

Hence, we deduce from (49) for all $\xi \in \mathcal{C} \setminus \mathcal{A}$ that

$$\epsilon \min\{\varepsilon_x/\lambda_{\max}(P),\, 2\min_i\, \nu_i,\, \min_i\, \vartheta_i\} \times \left(\lambda_{\max}(P)|x|^2 + \sum_{i=1}^{l} \left(\gamma_i \tilde{\phi}_i(\tau_i)|e_i|^2 + \eta_i \right) \right) \geqslant \sum_{i=1}^{l} \varepsilon_{y_i} \Delta_{0,i}^2. \tag{50}$$

Consequently, by using the fact that for $r \in \mathbb{N}$, $\min_{i\in\{1,2,\ldots,r\}} \alpha_i (\sum_{j=1}^{r} \beta_j) \leqslant \sum_{j=1}^{r} \alpha_j \beta_j$ for all $\alpha_j,\, \beta_j \in \mathbb{R}_{\geqslant 0}$, we can conclude that (48) indeed holds for all $\xi \in \mathcal{C} \setminus \mathcal{A}$. ■

Dynamics of U at jumps: In view of the jump map in (21), we distinguish two type of jumps.

1) When $\xi \in \mathcal{D}_i$ with $p_i = 0$, $i \in \{1, 2, \ldots, l\}$, and the system jumps according to $\xi^+ = G_i^\mu(\xi)$. This case corresponds to an update of the quantizer at node i. Since τ_i, e_i, and η_i are not affected by the jump map G_i^μ, we obtain

$$\begin{aligned} R(G(\xi)) - R(\xi) = {} & \gamma_i \tilde{\phi}_i(\tau_i^+)|e_i^+|^2 + \eta_i^+ \\ & - \gamma_i \tilde{\phi}_i(\tau_i)|e_i|^2 - \eta_i \overset{(21)}{=} 0. \end{aligned} \tag{51}$$

2) When $\xi \in \mathcal{D}_i$ with $p_i = 1$, $i \in \{1, 2, \ldots, l\}$, and the system jumps according to $\xi^+ = G_i^y(\xi)$. This case corresponds to a new transmission generated at some node i. In view of (20), (21) and by using the fact that $\tilde{\phi}(\tau_i^+) = \phi(\tau_i^+) = \lambda_i^{-1}$, we have that

$$\begin{aligned} R(G(\xi)) - R(\xi) &= \gamma_i \tilde{\phi}_i(\tau_i^+)|e_i^+|^2 + \eta_i^+ \\ &\quad - \gamma_i \tilde{\phi}_i(\tau_i)|e_i|^2 - \eta_i \\ &\overset{(21)}{=} \gamma_i \lambda_i^{-1} |e_{q,i}|^2 + \eta_{0,i}(e_i) - \gamma_i \tilde{\phi}_i(\tau_i)|e_i|^2 \\ &\overset{(10)}{\leqslant} \gamma_i \lambda_i^{-1} \Delta_i^2 \mu_i^2 + \eta_{0,i}(e_i) - \gamma_i \tilde{\phi}_i(\tau_i)|e_i|^2 \\ &\overset{(44)}{\leqslant} \gamma_i \lambda_i^{-1} \lambda_i^2 |e_i|^2 + \eta_{0,i}(e_i) - \gamma_i \tilde{\phi}_i(\tau_i)|e_i|^2 \\ &\overset{(25)}{=} \gamma_i \lambda_i |e_i|^2 + \gamma_i (\tilde{\lambda}_i - \lambda_i)|e_i|^2 - \gamma_i \tilde{\phi}_i(\tau_i)|e_i|^2 \\ &\overset{(28)}{\leqslant} \gamma_i \lambda_i |e_i|^2 + \gamma_i (\tilde{\lambda}_i - \lambda_i)|e_i|^2 - \gamma_i \tilde{\lambda}_i |e_i|^2 \leqslant 0. \end{aligned} \tag{52}$$

As a result, in view of (51) and (52), we have that when $\xi \in \mathcal{D}$, $R(G(\xi)) \leqslant R(\xi)$. In the view of the definition of $\mathcal{A}$, we also have that $G(\xi) \in \mathcal{A}$ when $\xi \in \mathcal{A}$. Given the latter facts, we can conclude that (46) holds for all $(t, j) \in \operatorname{dom} \xi$.

Dynamics of U during flows: Recall that $F(\xi, w) = (\mathcal{A}_1 x + \mathcal{B}_1 e + \mathcal{E}_1 w, \mathcal{A}_2 x + \mathcal{B}_2 e + \mathcal{E}_2 w, \mathbf{0}_l, \mathbf{1}_l, \Psi(o), \mathbf{0}_l)$. Consequently, in view of (20), (24), (28), we obtain for $\xi \in \mathcal{C}$ (recall that $\tilde{L}_i = L_i + \nu_i$, $i \in \{1, 2, \ldots, l\}$)

$$\begin{aligned} &\langle \nabla R, F(\xi, w) \rangle = \langle \nabla V(x), \mathcal{A}_1 x + \mathcal{B}_1 e + \mathcal{E}_1 w \rangle \\ &+ \sum_{i=1}^{l} 2\gamma_i \tilde{\phi}_i(\tau_i)|e_i| \left\langle \tfrac{\partial}{\partial e_i}|e_i|, \mathcal{A}_{2i} x + \mathcal{B}_{2i} e + \mathcal{E}_{2i} w \right\rangle \\ &+ \sum_{i=1}^{l} \gamma_i \dot{\tilde{\phi}}_i(\tau_i)|e_i|^2 + \sum_{i=1}^{l} \dot{\eta}_i \\ &\leqslant -\varepsilon_x |x|^2 - \sum_{i=1}^{l} |\mathcal{A}_{2i} x + \mathcal{B}_{2i} e + \mathcal{E}_{2i} w|^2 - \sum_{i=1}^{l} \varepsilon_{y_i} |y_i|^2 \\ &+ \sum_{i=1}^{l} \gamma_i^2 |e_i|^2 + \varepsilon_w |w|^2 + \sum_{i=1}^{l} 2L_i \gamma_i \tilde{\phi}_i(\tau_i)|e_i|^2 \\ &+ \sum_{i=1}^{l} 2\gamma_i \tilde{\phi}_i(\tau_i)|e_i||\mathcal{A}_{2i} x + \overline{\mathcal{B}}_{2i} e + \mathcal{E}_{2i} w| \\ &- \sum_{i=1}^{l} \tilde{\omega}_i(\tau_i) \left(2\tilde{L}_i \gamma_i \tilde{\phi}_i(\tau_i) + \gamma_i^2 (\tilde{\phi}_i^2(\tau_i) + 1) \right) |e_i|^2 \\ &+ \sum_{i=1}^{l} \tilde{\Psi}_i(y_i, e_i, \tau_i, \eta_i) \end{aligned}$$

for some $\tilde{\omega}_i(\tau_i) \in \omega_i(\tau_i)$ and $\tilde{\Psi}_i(y_i, e_i, \tau_i, \eta_i) \in \Psi_i(y_i, e_i, \tau_i, \eta_i)$.

By using the fact that $2\gamma_i \tilde{\phi}_i(\tau_i)|e_i||\mathcal{A}_{2i} x + \overline{\mathcal{B}}_{2i} e + \mathcal{E}_{2i} w| \leqslant \gamma_i^2 \tilde{\phi}_i^2(\tau_i)|e_i|^2 + |\mathcal{A}_{2i} x + \overline{\mathcal{B}}_{2i} e + \mathcal{E}_{2i} w|^2$ and since, in view of (25), $\Psi_i(y_i, e_i, \tau_i, \eta_i) \in \varepsilon_{y_i} \max\{|y_i|^2, \Delta_{0,i}^2\} - (1 - \omega_i(\tau_i))\tilde{\gamma}_i |e_i|^2 - \vartheta_i \eta_i$, we have that for all $\xi \in \mathcal{C}$

$$\begin{aligned} &\langle \nabla R, F(\xi, w) \rangle \leqslant -\varepsilon_x |x|^2 - \sum_{i=1}^{l} \varepsilon_{y_i} |y_i|^2 + \varepsilon_w |w|^2 \\ &+ \sum_{i=1}^{l} \left(2L_i \gamma_i \tilde{\phi}_i(\tau_i) + \gamma_i^2 (\tilde{\phi}_i^2(\tau_i) + 1) \right) |e_i|^2 \\ &- \sum_{i=1}^{l} \tilde{\omega}_i(\tau_i) \left(2\tilde{L}_i \gamma_i \tilde{\phi}_i(\tau_i) + \gamma_i^2 (\tilde{\phi}_i^2(\tau_i) + 1) \right) |e_i|^2 \\ &+ \sum_{i=1}^{l} \varepsilon_{y_i} \max\{|y_i|^2, \Delta_{0,i}^2\} - (1 - \tilde{\omega}_i(\tau_i))\tilde{\gamma}_i |e_i|^2 - \vartheta_i \eta_i \end{aligned}$$

for some $\tilde{\omega}_i(\tau_i) \in \omega_i(\tau_i)$.

By recalling that $\tilde{\gamma}_i = \gamma_i^2 + \gamma_i^2 \tilde{\lambda}_i^{\,2} + 2\gamma_i \tilde{\lambda}_i^{\,2} \tilde{L}_i$, $\tilde{L}_i = L_i + \nu_i$, and $\tilde{\phi}_i(\tau_i) = \phi_i(T_i) = \tilde{\lambda}_i$ for $\tau_i \geqslant T_i$ according to (28) and using the fact that $\max\{|y_i|^2, \Delta_{0,i}^2\} - |y_i|^2 \leqslant \Delta_{0,i}^2$, we obtain that $\langle \nabla R, F(\xi, w) \rangle \leqslant -\varepsilon_x |x|^2 + \sum_{i=1}^{l} \varepsilon_{y_i} \Delta_{0,i}^2 + \varepsilon_w |w|^2 - \sum_{i=1}^{l} 2\nu_i \gamma_i \tilde{\phi}_i(\tau_i)|e_i|^2 - \sum_{i=1}^{l} \vartheta_i \eta_i$. Now by means of Lemma 2, we obtain that for $\epsilon \in (0, 1)$ and for all $(t, j) \in \operatorname{dom} \xi$ for which $\xi(t, j) \in \mathcal{C} \setminus \mathcal{A}$, it holds that

$$\begin{aligned} \langle \nabla R, F(\xi, w) \rangle \leqslant {} & -(1 - \epsilon)\varepsilon_x |x|^2 + \varepsilon_w |w|^2 \\ & - (1 - \epsilon) \sum_{i=1}^{l} 2\nu_i \gamma_i \tilde{\phi}_i(\tau_i)|e_i|^2 - (1 - \epsilon) \sum_{i=1}^{l} \vartheta_i \eta_i. \end{aligned} \tag{53}$$

By recalling the fact that $U(\xi) = 0$ when $\xi \in \mathcal{A}$, we can conclude that for all $(t, j) \in \operatorname{dom} \xi$ for which $\xi(t, j) \in \mathcal{C}$

$$\langle \nabla U(\xi, F(\xi, w)) \rangle \leqslant -\rho U(\xi) + \varepsilon_w |w|^2 \tag{54}$$

where $\rho := (1 - \epsilon) \min\{\frac{\varepsilon_x}{\lambda_{\max}(P)}, 2\min_i\, \nu_i, \min_i\, \vartheta_i\}$ and thus, that (47) holds.

t-completeness of maximal solutions: We investigate t-completeness of maximal solutions. To do so, we verify the conditions provided in [29, Prop. 6.10]. First of all, observe that $G(\mathcal{D}) \subset \mathcal{C} \cup \mathcal{D}$, since for all $\xi \in G(\mathcal{D})$, it holds that $\tau_i^+ \geqslant 0$, $\eta_i^+ \geqslant 0$, $\mu_i^+ \geqslant \frac{\Omega_{\text{in},i}}{\ell_{\text{in},i}} \Delta_{0,i}$, and $p_i^+ \in \{0, 1\}$ due to

(20), (25), and property (d) below (38). Next, we show that for any $\varphi \in \mathcal{C}\backslash\mathcal{D}$ there exists a neighborhood S of ξ such that, it holds for every $\varphi \in S \cap \mathcal{C}$ that $F(\varphi, w) \cap T_{\mathcal{C}}(\varphi) \neq \emptyset$, where $T_{\mathcal{C}}(\varphi)$ is the tangent cone[5] to $\mathcal{C}$ at φ. Observe that for each $\xi \in \mathcal{C}$ (recall that $\xi = (x, e, \mu, \tau, \eta, p)$), $T_{\mathcal{C}}(\xi) = \mathbb{R}^{n_x} \times \mathbb{R}^{n_y} \times (T_{\mathbb{R}_{\geqslant \underline{\mu}_1}}(\mu_1) \times \cdots \times T_{\mathbb{R}_{\geqslant \underline{\mu}_l}}(\mu_l)) \times (T_{\mathbb{R}_{\geqslant 0}}(\tau_1) \times \cdots \times T_{\mathbb{R}_{\geqslant 0}}(\tau_l)) \times (T_{\mathbb{R}_{\geqslant 0}}(\eta_1) \times \cdots \times T_{\mathbb{R}_{\geqslant 0}}(\eta_l)) \times \{0\}^l$. Observe also from (19) that $\mathcal{C}/\mathcal{D} = \bigcap_{i=1}^{l} \{\xi \in \mathbb{X} : p_i = 0 \text{ and } (\tau_i < T_i \text{ or } \eta_i > 0)\}$. Given the facts that, for all $i \in \{1, 2, \ldots, l\}$, $\dot{\tau}_i = 1$ and $\dot{\mu}_i = 0$ due to (21) and that $\dot{\eta}_i > 0$ when $\tau_i < T_i$ and $\eta_i = 0$ due to (9) and (25), it indeed follows that for any $\xi \in \mathcal{C}\backslash\mathcal{D}$ there exists a neighborhood S of ξ such that, it holds for every $\varphi \in S \cap \mathcal{C}$ that $F(\varphi, w) \cap T_{\mathcal{C}}(\varphi) \neq \emptyset$. To conclude the proof for t-completeness, finite escape times should be excluded which is the case due to (47). Hence, indeed all maximal solutions (20), (21) with $\xi(0, 0) \in \mathbb{X}_0$ and $w \in \mathcal{L}_\infty$ are t-complete.

Proof of statement 2: To obtain the upper bound for $\kappa_{\text{out},i}(y_i, \mu_i)$, we first derive an upper bound for y_i. From (54), we obtain that

$$U(\xi(t, j)) \leqslant e^{-\rho t} U(\xi(0, 0)) + \varepsilon_w \int_0^t e^{-\rho(t-s)} |w(s)|^2 ds.$$

By combining the latter with the fact that $U(\xi(t, j)) \geqslant x^\top(t, j) Px(t, j) - c \geqslant \frac{\lambda_{\min}(P)}{\lambda_{\max}(C_{p,i}^\top C_{p,i}) y(t,j)} - c$, we can conclude that $\|y_i\|_\infty \leqslant \bar{y}_i$ with $\bar{y}_i$ as in (39). Consequently, in view of (31) and the fact $\mu_i(t, j) \geqslant \underline{\mu}_i$ for all $(t, j) \in \operatorname{dom} \xi$, we can conclude that the elements of $\kappa_{\text{out},i}(y_i, \mu_i)$ are upper bounded by $\kappa^*_{\text{out},i}$ as in (36).

To obtain the upper bound for $\kappa_{\text{in},i}(y_i, \mu_i)$, we first derive an upper bound for μ_i. By recalling the fact that μ_i, $i \in \{1, 2, \ldots, l\}$, is only increased when $|y_i| \geqslant \ell_{\text{out},i} \mu_i$ (see also property (b) below (38), we obtain that $\|\mu_i\|_\infty \leqslant \bar{\mu}_i$ with $\bar{\mu}_i$ as in (37). Given the latter, we can obtain from (31) that the elements of $\kappa_{\text{in},i}(y_i, \mu_i)$ are upper bounded by $\kappa^*_{\text{in},i}$ as in (35).

All the statements of Theorem 1 are now proved. ■

REFERENCES

[1] J. Baillieul and P. J. Antsaklis, "Control and communication challenges in networked real-time systems," *Proc. IEEE*, vol. 95, no. 1, pp. 9–28, Jan. 2007.

[2] W. P. M. H. Heemels, A. R. Teel, N. van de Wouw, and D. Nešić, "Networked control systems with communication constraints: Tradeoffs between transmission intervals, delays and performance," *IEEE Trans. Autom. Control*, vol. 55, no. 8, pp. 1781–1796, Aug. 2010.

[3] A. S. Matveev and A. V. Savkin, *Estimation and Control over Communication Networks*. Basel, Switzerland: Birkhäuser, 2009.

[4] W. P. M. H. Heemels, K. H. Johansson, and P. Tabuada, "An introduction to event-triggered and self-triggered control," in *Proc. 51st IEEE Conf. Decis. Control*, Maui, HI, USA, 2012, pp. 3270–3285.

[5] R. Postoyan, P. Tabuada, D. Nešić, and A. Anta, "A framework for the event-triggered stabilization of nonlinear systems," *IEEE Trans. Autom. Control*, vol. 60, no. 4, pp. 982–996, Apr. 2015.

[5]The tangent cone to a set $S \subset \mathbb{R}^n$ at a point $x \in \mathbb{R}^n$, denoted $T_S(x)$, is the set of all vectors $\omega \in \mathbb{R}^n$ for which there exist $x_i \in S, \tau_i > 0$ with $x_i \to x, \tau \to 0$ as $i \to \infty$ such that $\omega = \lim_{i\to\infty}(x_i - x)/\tau_i$ (see [29, Def. 5.12]).

[6] S. Tarbouriech, A. Seuret, J. M. G. da Silva Jr., and D. Sbarbaro, "Observer-based event-triggered control co-design for linear systems," *IET Control Theory Appl.*, vol. 10, no. 18, pp. 2466–2473, 2016.

[7] M. C. F. Donkers and W. P. M. H. Heemels, "Output-based event-triggered control with guaranteed $\mathcal{L}_\infty$-gain and improved and decentralized event-triggering," *IEEE Trans. Autom. Control*, vol. 57, no. 6, pp. 1362–1376, Jun. 2012.

[8] D. P. Borgers and W. P. M. H. Heemels, "Event-separation properties of event-triggered control systems," *IEEE Trans. Autom. Control*, vol. 59, no. 10, pp. 2644–2656, Oct. 2014.

[9] D. Nešić and D. Liberzon, "A unified framework for design and analysis of networked and quantized control systems," *IEEE Trans. Autom. Control*, vol. 54, no. 4, pp. 732–747, Apr. 2009.

[10] W. P. M. H. Heemels, D. Nešić, and A. R. Teel, "Networked and quantized control systems with communication delays," in *Proc. Joint 48th IEEE Conf. Decis. Control 28th Chin. Control Conf.*, Shanghai, China, 2009, pp. 7929–7935.

[11] L. A. Montestruque and P. J. Antsaklis, "Static and dynamic quantization in model-based networked control systems," *Int. J. Control*, vol. 80, no. 1, pp. 87–101, 2007.

[12] H. Fujioka, "Stability analysis for a class of networked/embedded control systems: A discrete-time approach," in *Proc. Amer. Control Conf.*, Washington, WA, USA, 2008, pp. 4997–5002.

[13] D. Liberzon, "Quantization, time delays, and nonlinear stabilization," *IEEE Trans. Autom. Control*, vol. 51, no. 7, pp. 1190–1195, Jul. 2006.

[14] S. J. L. M. van Loon, M. C. F. Donkers, N. van de Wouw, and W. P. M. H. Heemels, "Stability analysis of networked and quantized linear control systems," *Nonlinear Anal., Hybrid Syst.*, vol. 10, pp. 111–125, 2013.

[15] R. W. Brockett and D. Liberzon, "Quantized feedback stabilization of linear systems," vol. 45, no. 7, pp. 1279–1289, 2000.

[16] D. Liberzon and D. Nešić, "Input-to-state stabilization of linear systems with quantized state measurements," *IEEE Trans. Autom. Control*, vol. 52, no. 5, pp. 767–781, May 2007.

[17] P. Tabuada, "Event-triggered real-time scheduling of stabilizing control tasks," *IEEE Trans. Autom. Control*, vol. 52, no. 9, pp. 1680–1685, Sep. 2007.

[18] P. Tallapragada and J. Cortes, "Event-triggered stabilization of linear systems under bounded bit rates," *IEEE Trans. Autom. Control*, vol. 61, no. 6, pp. 1575–1589, Jun. 2016.

[19] T. Liu and Z. Jiang, "Quantized event-based control of nonlinear systems," in *Proc. 54th IEEE Conf. Decis. Control*, Osaka, Japan, 2015, pp. 4806–4811.

[20] L. Li, X. Wang, and M. Lemmon, "Stabilizing bit-rate of perturbed event triggered control systems," in *Proc. 4th IFAC Conf. Anal. Design Hybrid Syst.*, Eindhoven, Netherlands, 2012, pp. 70–75.

[21] Y. Sun and X. Wang, "Stabilizing bit-rates in networked control systems with decentralized event-triggered communication," *Discrete Event Dyn. Syst.*, vol. 24, pp. 219–245, 2014.

[22] A. Tanwani, C. Prieur, and M. Fiacchini, "Observer-based feedback stabilization of linear systems with event-triggered sampling and dynamic quantization," *Syst. Control Lett.*, vol. 94, pp. 46–56, 2016.

[23] J. R. Ramirez, Y. Minami, and K. Sugimoto, "Event-triggered dynamic quantizers for networked control systems," in *Proc. 20th IFAC World Congr.*, Toulouse, France, 2017, pp. 5190–5195.

[24] J. He, Q. Ma, J. Guo, and C. Zhou, "Event-triggered mechanism based dynamic quantized output feedback controller for networked control systems," in *Proc. 29th Chin. Control Decis. Conf.*, Chongqing, China, 2017, pp. 2569–2574.

[25] V. S. Dolk, D. P. Borgers, and W. P. M. H. Heemels, "Output-based and decentralized dynamic event-triggered control with guaranteed $\mathcal{L}_p$-gain performance and Zeno-freeness," *IEEE Trans. Autom. Control*, vol. 62, no. 1, pp. 34–49, Jan. 2017.

[26] M. Abdelrahim, R. Postoyan, J. Daafouz, and D. Nešić, "Stabilization of nonlinear systems using event-triggered output feedback laws," *IEEE Trans. Autom. Control*, vol. 61, no. 9, pp. 2682–2687, Sep. 2016.

[27] A. Girard, "Dynamic triggering mechanisms for event-triggered control," *IEEE Trans. Autom. Control*, vol. 60, no. 7, pp. 1992–1997, Jul. 2015.

[28] M. Abdelrahim, V. S. Dolk, and W. P. M. H. Heemels, "Input-to-state stabilizing event-triggered control for linear systems with output quantization," in *Proc. 55th IEEE Conf. Decis. Control*, Las Vegas, CA, USA, 2016, pp. 483–488.

[29] R. Goebel, R. G. Sanfelice, and A. R. Teel, *Hybrid Dynamical Systems: Modeling, Stability, and Robustness*. Princeton, NJ, USA: Princeton Univ. Press, 2012.

[30] C. Cai and A. R. Teel, "Characterizations of input-to-state stability for hybrid systems," *Syst. Control Lett.*, vol. 58, no. 1, pp. 47–53, 2009.
[31] D. Nešić, A. R. Teel, G. Valmorbida, and L. Zaccarian, "Finite-gain $\mathcal{L}_p$ stability for hybrid dynamical systems," *Automatica*, vol. 49, no. 8, pp. 2384–2396, 2013.
[32] T. Arampatzis, J. Lygeros, and S. Manesis, "A survey of applications of wireless sensors and wireless sensor networks," in *Proc. IEEE Int. Symp. Mediterrean Conf. Control Autom. Intell. Control*, Limassol, Cyprus, 2005, pp. 719–724.
[33] D. Liberzon, "Hybrid feedback stabilization of systems with quantized signals," *Automatica*, vol. 39, no. 9, pp. 1543–1554, 2003.
[34] T. Kameneva and D. Nešić, "Robustness of quantized control systems with mismatch between coder/decoder initializations," *Automatica*, vol. 45, no. 3, pp. 817–822, 2009.
[35] C. de Persis and A. Isidori, "Stabilizability by state feedback implies stabilizability by encoded state feedback," *Syst. Control Lett.*, vol. 53, no. 3/4, pp. 249–258, 2004.
[36] A. R. Teel and D. Nešić, "Lyapunov functions for $\mathcal{L}_2$ and input-to-state stability in a class of quantized control systems," in *Proc. 50th IEEE Conf. Decis. Control Eur. Control Conf.*, Orlando, FL, USA, 2011, pp. 4542–4547.
[37] M. Abdelrahim, R. Postoyan, and J. Daafouz, "Event-triggered control of nonlinear singularly perturbed systems based only on the slow dynamics," *Automatica*, vol. 52, pp. 15–22, 2015.
[38] V. S. Dolk and W. P. M. H. Heemels, "Event-triggered control under packet losses," *Automatica*, vol. 80, pp. 143–155, 2017.
[39] Y. Sharon and D. Liberzon, "Input to state stabilizing controller for systems with coarse quantization," *IEEE Trans. Autom. Control*, vol. 57, no. 4, pp. 830–844, Apr. 2012.
[40] T. M. Cheng, "Robust stabilisation of nonlinear systems using output measurements via finite data-rate communication channels," in *Proc. 44th IEEE Conf. Decis. Control*, Seville, Spain, 2005, pp. 866–871.
[41] P. Shi, H. Wang, and C. Lim, "Network-based event-triggered control for singular systems with quantizations," *IEEE Trans. Ind. Electron.*, vol. 63, no. 2, pp. 1230–1238, Feb. 2016.
[42] F. Qu, Z. Guan, D. He, and M. Chi, "Event-triggered control for networked control systems with quantization and packet losses," *J. Franklin Inst.*, vol. 352, pp. 974–986, 2015.
[43] D. Carnevale, A. R. Teel, and D. Nešić, "A Lyapunov proof of an improved maximum allowable transfer interval for networked control systems," *IEEE Trans. Autom. Control*, vol. 52, no. 5, pp. 892–897, May 2007.
[44] M. Abdelrahim, R. Postoyan, J. Daafouz, and D. Nešić, "Robust event-triggered output feedback controllers for nonlinear systems," *Automatica*, vol. 75, pp. 96–108, 2017.
[45] J. Zhang and G. Feng, "Event-driven observer-based output feedback control for linear systems," *Automatica*, vol. 50, pp. 1852–1859, 2014.
[46] M. Abdelrahim, R. Postoyan, J. Daafouz, and D. Nešić, "Co-design of output feedback laws and event-triggering conditions for linear systems," in *Proc. 53rd IEEE Conf. Decis. Control*, Los Angeles, CA, USA, 2014, pp. 3560–3565.
[47] W. P. M. H. Heemels and S. Weiland, "Input-to-state stability and interconnections of discontinuous dynamical systems," *Automatica*, vol. 44, no. 12, pp. 3079–3086, 2008.
[48] C. Prieur, A. R. Teel, and L. Zaccarian, "Relaxed persistent flow/jump conditions for uniform global asymptotic stability," *IEEE Trans. Autom. Control*, vol. 59, no. 10, pp. 2766–2771, Oct. 2014.

Mahmoud Abdelrahim (M'16) received the M.Sc. degree in mechatronics engineering from Assiut University, Asyut, Egypt, in 2010. He obtained the Ph.D. degree in control theory from the Centre de Recherche en Automatique de Nancy (CRAN), Université de Lorraine, France in 2014.

From September 2014 to June 2015 he was a Research and Teaching Assistant with the Université de Lorraine, France. From July 2015 to October 2016, he was a Postdoctoral Researcher with the Department of Mechanical Engineering, Eindhoven University of Technology (TU/e), The Netherlands. Since November 2016, he has been with the Department of Mechanical Engineering, Assiut University, Egypt, where he is currently a Lecturer with the Mechatronics section.

His research interests include event-triggered control, networked control systems, hybrid dynamical systems, robust stabilization, and optimization.

Victor Sebastiaan Dolk (S'14) received the M.Sc. and Ph.D. degrees (cum laude) in mechanical engineering from the Eindhoven University of Technology (TU/e), Eindhoven, the Netherlands.

In 2013, he joined ASML, Research Department, in Veldhoven, The Netherlands. His research interests include hybrid dynamical systems, networked control systems, intelligent transport systems, model predictive control, and event-triggered control.

W. P. M. H. Heemels (F'06) received the M.Sc. degree in mathematics and the Ph.D. degree in control theory (both summa cum laude) from the Eindhoven University of Technology (TU/e), Eindhoven, The Netherlands, in 1995 and 1999, respectively.

From 2000 to 2004, he was an Assistant Professor with the Electrical Engineering Department, TU/e, and from 2004 to 2006, a Research Fellow with the Embedded Systems Institute (ESI). Since 2006, he has been with the Department of Mechanical Engineering, TU/e, where he is currently a Full Professor in the Control Systems Technology Group. He has held Visiting Professor positions with the Swiss Federal Institute of Technology (ETH), Zurich, Switzerland (2001) and with the University of California at Santa Barbara (2008). In 2004, he was also at the Research and Development Laboratory, Océ, Venlo, The Netherlands. His current research interests include hybrid and cyber-physical systems, networked and event-triggered control systems and constrained systems including model predictive control.

Dr. Heemels served/s on the editorial boards of IEEE TRANSACTIONS ON AUTOMATIC CONTROL, *Automatica*, *Nonlinear Analysis: Hybrid Systems and Annual Reviews in Control*. He was a recipient of a personal VICI grant awarded by NWO (The Netherlands Organisation for Scientific Research) and STW (Dutch Technology Foundation).